Journal of Orthopaedic Translation 46 (2024) 1–17

Contents lists available at ScienceDirect

Journal of Orthopaedic Translation

journal homepage: www.journals.elsevier.com/journal-of-orthopaedic-translation

Original articel

Sipeimine ameliorates osteoarthritis progression by suppression of NLRP3 inflammasome-mediated pyroptosis through inhibition of PI3K/AKT/NF-κB pathway: An in vitro and in vivo study

Yuqin Fang [a,b,c,1], Chao Lou [a,b,c,1], Junlei Lv [a,b,c,1], Chaoyang Zhang [a,b,c], Ziteng Zhu [a,b,c], Wei Hu [a,b,c], Hua Chen [a,b,c,***], Liaojun Sun [a,b,c,**], Wenhao Zheng [a,b,c,*]

[a] Department of Orthopaedics, The Second Affiliated Hospital and Yuying Children's Hospital of Wenzhou Medical University, Wenzhou, 325000, China
[b] Key Laboratory of Orthopaedics of Zhejiang Province, Wenzhou, 325000, China
[c] The Second School of Medicine of Wenzhou Medical University, Wenzhou, 325000, China

ARTICLE INFO

Keywords:
NLRP3
Osteoarthritis
PI3K
Pyroptosis
Sipeimine

ABSTRACT

Background: Osteoarthritis (OA) is a chronic and degenerative condition that persists and progresses over time. Sipeimine (Sip), a steroidal alkaloid derived from *Fritillariae Cirrhosae Bulbus*, has attracted considerable attention due to its exceptional anti-inflammatory, analgesic, antioxidant, and anti-cancer characteristics. However, Sip's effects on OA and its mechanism still need further research.

Methods: This study utilized network pharmacology to identify initial targets for Sip. Functional associations of Sip in OA were clarified through Gene Ontology (GO) enrichment analysis, bioinformatically analyzing a list of targets. Subsequently, Kyoto Encyclopedia of Genes and Genomes (KEGG) enrichment analysis assessed pathways linked to Sip's therapeutic efficacy in OA. Molecular docking techniques explored Sip's binding affinity with key targets. In vitro experiments assessed Sip's impact on lipopolysaccharide (LPS)-induced pro-inflammatory factors and its protective effects on collagen-II and aggrecan degradation within the extracellular matrix (ECM). Western blotting and fluorescence analyses were conducted to determine Sip-mediated signaling pathways. Moreover, in vivo experiments using a mouse OA model validated Sip's therapeutic efficacy.

Results: The results from network pharmacology revealed a total of 57 candidate targets for Sip in OA treatment. GO enrichment analysis demonstrated a robust correlation between Sip and inflammatory response, response to LPS and NF-κB-inducing kinase activity in OA. KEGG enrichment analysis highlighted the significance of NF-κB and PI3K-AKT pathways in Sip's therapeutic potential for OA. Furthermore, molecular docking results demonstrated Sip's robust binding affinity with p65 and PI3K. In vitro experiments demonstrated Sip's effectively suppressed the expression of pro-inflammatory factors induced by LPS, such as COX-2, iNOS, IL-1β, and IL-18. Besides, Sip counteracted the degradation of collagen-II and aggrecan within the ECM and the expression of MMP-13 and ADAMTS-5 mediated by LPS. The safeguarding effects of Sip were ascribed to its inhibition of PI3K/AKT/NF-κB pathway and NLRP3 inflammasome mediated pyroptosis. Additionally, in vivo experiments revealed that Sip could alleviate the subchondral remodeling, cartilage degeneration, synovitis as well as ECM degradation a mouse model of OA.

Conclusion: Sip exhibited potential in attenuating OA progression by suppressing the PI3K/AKT/NF-κB pathway, consequently inhibiting the activation of NLRP3 inflammasome and pyroptosis.

* Corresponding author. Department of Orthopaedics, The Second Affiliated Hospital and Yuying Children's Hospital of Wenzhou Medical University, 109 West Xueyuan Road, Wenzhou, Zhejiang Province, 325027, China.
** Corresponding author. Department of Orthopaedics, The Second Affiliated Hospital and Yuying Children's Hospital of Wenzhou Medical University, 109 West Xueyuan Road, Wenzhou, Zhejiang Province, 325027, China.
*** Corresponding author. Department of Orthopaedics, The Second Affiliated Hospital and Yuying Children's Hospital of Wenzhou Medical University, 109 West Xueyuan Road, Wenzhou, Zhejiang Province, 325027, China.
E-mail addresses: chenhuafey@126.com (H. Chen), sunlj797110@163.com (L. Sun), zhengwenhao@wmu.edu.cn (W. Zheng).
[1] These authors contributed equally: Yuqin Fang, Chao Lou and Junlei Lv.

https://doi.org/10.1016/j.jot.2024.04.004
Received 4 January 2024; Received in revised form 29 February 2024; Accepted 23 April 2024
Available online 9 May 2024

The translational potential statement: The translational potential of this articleThis study provides a biological rationale for the use of Sip as a potential candidate for OA treatment, provide a new concept for the cartilage targeted application of natural compounds.

1. Introduction

Osteoarthritis (OA) is evident through an enduring degenerative arthropathy marked by the deterioration of cartilage, inflammatory response, reduction of joint space and the development of osteophytes [1]. These pathological changes may result in articular synovitis, varus deformity, meniscus rupture and potentially lead to disability [2]. The risk factors associated with OA encompass aging, trauma, obesity, and genetic predisposition [3]. Furthermore, OA is closely entwined with the inflammatory cascade, instigating cellular alterations, structural impairments, and functional disturbances in cartilage, bone, and synovium [4]. Numerous investigations have confirmed a strong association between inflammatory cytokines and the onset and advancement of OA [5]. Notably, a pivotal role in the inflammatory cascade of OA is played by interleukin-1β (IL-1β), triggering the overexpression of pertinent catabolic enzymes and inflammatory mediators, such as prostaglandin E2 (PGE2), nitric oxide (NO), matrix metalloproteinases (MMPs) and a disintegrin and metalloproteinase with thrombospondin motifs (ADAMTS), collectively contributing to the degradation of the extracellular matrix (ECM) [6,7]. Moreover, reports substantiate the abnormal elevation of inflammatory mediators, such as IL-1β, IL-6 and tumor necrosis factor-α (TNF-α), within the synovial membrane, synovial fluid, and cartilage of individuals afflicted with OA, underscoring the pivotal roles that these mediators assume in the pathogenesis of OA [8]. These revelations spotlight the potential of agents aimed at countering inflammatory mediators as promising avenues in the therapeutic repertoire for OA management.

Pyroptosis is a programmed cell death signal pathway mediated by the caspase-1-required inflammasome, leading to the production of IL-18 and IL-1β, along with the lysis of macrophage cells [9]. Diverging from apoptosis and conventional cell necrosis, pyroptosis emerges as a proinflammatory process regulated by the caspase-1 signaling and nod-like receptor protein-3 (NLRP3) inflammasome. The activation of the inflammasome results in caspase-1 cleavage, facilitating the maturation and subsequent release of IL-18 and IL-1β, effectively regulating the inflammatory process [10]. Moreover, the detection of heightened levels of NLRP3, IL-18, and IL-1β in the synovial membrane of rats afflicted with knee osteoarthritis indicates the involvement of the inflammasome in the pathogenesis of OA [11]. Studies conducted previously have affirmed the critical activation role of the nuclear factor-κB (NF-κB) pathway in the inflammatory response as well as the progression of OA [12,13]. The initiation of the NLRP3 inflammasome is dependent on the NF-κB pathway [14]. During the initiation and advancement of OA, NF-κB can activate NLRP3 and initiate pyroptosis of chondrocyte, thereby release more IL-18 and IL-1β, which accelerates the progression of OA [15]. The phosphatidylinositol 3 kinase (PI3K)/-protein kinase B (AKT) signaling pathway is involved in the occurrence and progression of many inflammatory diseases including OA [16]. The activation of the PI3K/AKT pathway induces the downstream substrate NF-κB, leading to phosphorylation of i-κBα and p65, which promotes overexpression of inflammatory mediators in chondrocytes and aggravates the progression of OA [17]. Therefore, the PI3K/AKT/NF-κB/NLRP3-mediated pyroptosis pathway is crucial in OA progression and is acknowledged as a primary target for therapeutic intervention in OA.

Natural herbs and their bioactive compounds, possessing therapeutic attributes, have proven effective against OA and have become the focus of extensive research. *Fritillariae Cirrhosae Bulbus* belongs to the *Fritillaria* genus in the *Liliaceae* family and is mainly found in Southwestern China, is traditionally employed in Chinese medicine for treating diseases like asthma, inflammation, and tumors [18]. The principal active compounds of *Fritillariae Cirrhosae Bulbus* are alkaloids, manifesting diverse effects such as expectorant, cough suppressant, anti-inflammatory, analgesic, antioxidant, and anti-cancer properties [19,20]. Sipeimine (Sip, also known as imperialine), a steroidal alkaloid derived from *Fritillariae Cirrhosae Bulbus*, manifests various pharmacological benefits, encompassing anti-asthmatic activity [19], anti-hypotensive effects [21], anti-tumor properties [22], as well as anti-inflammatory and antibacterial activities [23]. In RAW 264.7 macrophages stimulated with lipopolysaccharide (LPS), Sip exhibited the inhibition of pro-inflammatory mediators, including NO, IL-1β, TNF-α, inducible nitric oxide synthase (iNOS), cyclooxygenase-2 (COX-2), as well as NF-κB [24]. Moreover, in the context of PM2.5-induced lung toxicity, Sip mitigated damage and NLRP3 inflammasome-mediated pyroptosis by regulating the PI3K/AKT signaling pathway [25]. Concurrently, in rats with PM2.5-induced lung injury, Sip exhibited a protective effect by suppressing ferroptosis through modulation of the PI3K/AKT/Nrf2 signaling pathway [26]. Additionally, in a rat model resembling chronic obstructive pulmonary disease (COPD), Sip mitigated both functional and structural pulmonary impairment, concurrently suppressing the inflammatory response. This outcome was accomplished through the modulation of the expression of relevant inflammatory cytokines (IL-1β, IL-8, IL-6, NF-κB, TNF-α and TGF-β1) in the lung tissues of the COPD-like rats [23]. While previous studies have delved into the protective mechanisms of Sip, its precise role and mechanisms in alleviating the progression of OA remain an uncharted territory in scientific exploration.

The study aims to explore the potential benefits of Sip in alleviating the LPS-induced degradation of the ECM and the correlated inflammatory response in chondrocytes. Additionally, the study seeks to evaluate Sip's protective effects in OA animal models induced via medial meniscus surgical destabilization. Moreover, the research aims to uncover unrevealed molecular mechanisms contributing to its anti-inflammatory properties in both in vitro and in vivo settings.

2. Materials and methods

2.1. Animal model and experimental design

Forty-five male C57BL/6 mice, aged 8–10 weeks, were procured from the Animal Center of the Chinese Academy of Sciences in Shanghai, China. Approval for the ethical treatment and use of experimental animals, adhering to the guidelines stipulated in the National Institutes of Health's Care and Use of Laboratory Animals, was granted by the Animal Care and Use Committee of Wenzhou Medical University (ethic code: wydw2023-0310). The mice were randomly assigned to three groups (15 mice in each group): sham, DMM, and DMM + Sip, using a randomization procedure. For standardization, mice received intraperitoneal anesthesia with a 2 % (w/v) pentobarbital solution at a dosage of 40 mg/kg. The generation of OA murine models involved a surgical procedure encompassing the precise transection of the medial meniscotibial ligaments, executed through incisions thoughtfully situated in the joint capsules of the right knee, positioned medially to the patellar tendon. In contrast, the mice within the sham group underwent an arthrotomy procedure devoid of any intervention on the medial meniscotibial ligaments. Across a 14-day duration, the DMM + Sip group underwent daily intra-articular injections of Sip (30 mg/kg), dissolved in saline with 0.1 % dimethyl sulfoxide (DMSO), whereas both the DMM and sham groups were administered equivalent daily volumes of saline. The Sip dosage was determined from available literature [26].

After an 8-week period, mice got humanely euthanized, and samples of knee joints got harvested for micro-computed tomography scans and histological assessments.

2.2. Reagents

Chengdu Munster Co., Ltd. (Chengdu, China) supplied Sipeimine (purity ≥98 %). Dojindo (Kumamo, Japan) supplied the Cell-Counting Kit-8 (CCK-8) assays. Primary antibodies targeting proteins IκBα (#ab32518), MMP-13 (#ab39012), ASC (#ab309497), NLRP3 (#ab263899), caspase-1 (#ab138483), aggrecan (#ab216965), ADAMTS-5 (#ab41037), Lamin B (#ab16048), collagen-II (#ab34712) were meticulously procured from Abcam (Cambridge, MA, USA). Sigma Chemical Co. (St. Louis, MO, USA) supplied collagenase II. Additional primary antibodies p65 (#8242), p-p65 (#3033), Gasdermin D (#39754), cleaved-Gasdermin D(#10137), cleaved-caspase-1 (#89332), p-IκBα (#9246), PI3K (#4249), P-PI3K (#4228), P-AKT (#9271), AKT (#9272), COX-2 (#12282), iNOS (#13120), GAPDH (#2118) were contributed by Cell Signaling Technology (MA, USA). For immunofluorescence labeling, secondary antibodies (Alexa Spectrum®594-conjugated and Alexa Spectrum®488-tagged) were chosen from Jackson ImmunoResearch (West Grove, PA, USA). Essential enzyme-linked immunosorbent assay (ELISA) kits of IL-1β (#MLB00C), IL-18 (#DY7625-05), nitrite (#KGE001) and PGE2 (#KGE004B) were furnished by R&D Systems (Minneapolis, MN, USA), and Fetal Bovine Serum (FBS) along with Dulbecco's Modified Eagle's Medium (DMEM)/Ham's F12 medium were provided by Gibco (Grand Island, NY, USA).

2.3. Network pharmacology

From the PubChem database, we extracted the molecular structure of Sip's bioactive constituents. Simultaneously, we identified its target using the SwissTarget Prediction database and illustrated Sip's chemical structure. The online repository GeneCards was then employed to identify targets associated with the ailment. Using the Cytoscape software, we executed the creation of a model that integrated the disease, drug constituents and their targets. Moreover, using STRING software, we constructed a protein–protein interactions (PPI) network. The R software was utilized to conduct comprehensive analyses, including Kyoto Encyclopedia of Genes and Genomes (KEGG) and Gene Ontology (GO) enrichment analysis.

2.4. Molecular docking

Details regarding molecular mass, chemical nomenclature and 3D configuration were sourced from the PubChem repository. Moreover, from the RCSB PDB database (accessible at http://www.rcsb.org/), 3D structures associated with the activation of PI3K (PDB ID: 1E7U) and p65 (PDB ID: 8GAP) proteins were obtained. For molecular docking facilitation, protein setup and ligand utilized the AutoDock Vina software (available at http://vina.scripps.edu/). In preparing the crystal structures of the target biomarker, crucial tasks included eliminating amino acid adjustments, water molecules, hydrogenation, and eliminating force field while fine-tuning energy parameters. Achieving the criteria for the ligand's low-energy conformation was an essential prerequisite. Following this, the Vina program integrated into Pyrx software was employed for the molecular docking of the target structure with the active compound. Quantifying the interaction strength between the two entities was done by measuring the binding affinity, denoted in kcal/mol. It is important to highlight that a lower binding affinity signifies a more robust and stable ligand–receptor interaction. The results of the docking procedure underwent careful scrutiny and were visualized using Discovery Studio and Pymol software.

Table 1
The sequence of qRT-PCR..

Gene	Forward primer	Reverse primer
IL-1β	5′-CTTCAGGCAGGCAGTATCACTC-3′	5′-TGCAGTTGTCTAATGGGAACGT-3′
COX-2	5′-TCCTCACATCCCTGAGAACC-3′	5′-GTCGCACACTCTGTTGTGCT-3′
iNOS	5′-GACGAGACGGATAGGCAGAG-3′	5′-CACATGCAAGGAAGGGAACT-3′
IL-18	5′-GCCTCAAACCTTCCAAATCA-3′	5′-TGGATCCATTTCCTCAAAGG-3′

2.5. Primary mouse chondrocyte culture

Knee cartilage from C57BL/6 neonatal mice (3–5 days old) was used to isolate chondrocytes. Small fragments of the cartilaginous tissue specimens were dissected, followed by three consecutive washes with PBS. Subsequently, the dissected fragments were enzymatically processed with collagenase-II (2 mg/ml) at 37 °C for 4 h. Following centrifugation and a rinse with PBS, chondrocytes were cultured in a controlled environment at 37 °C with 5 % CO2. The employed culture medium consisted of DMEM/F12 supplemented with 1 % penicillin/streptomycin and 10 % FBS. Chondrocytes in the 2nd passage were utilized for all subsequent experimental procedures, and the culture medium was replaced daily throughout the culture period.

2.6. Cell viability assays

The response of mouse chondrocytes to the cytotoxic effects of Sip was assessed using a CCK-8 assay according to the manufacturer's protocol (Dojindo, Japan). In the initial step of the experimental procedure, second-passage chondrocytes were plated in 96-well microplates at a density of 8000 cells/well. Chondrocytes were treated with varying concentrations of Sip (0, 10, 25, 50, 100, and 200 μM) after incubating for 24 and 48 h. Following exposure to Sip, a 10 μL aliquot of CCK-8 reagent was applied to each well, and microplates underwent a 2 h incubation at 37 °C. Spectrophotometric measurements were then recorded at a wavelength of 450 nm for the optical density (OD). To ensure the reliability of the results, all experiments were systematically conducted in triplicate.

2.7. ELISAs

Culture supernatants from the treatment of OA chondrocytes were analyzed for IL-18, IL-1β, PGE2 and nitrite levels using a commercial ELISA kit (R&D Systems, Minneapolis, MN, USA) following specific recommendations. The analysis was conducted in triplicate for the assay.

2.8. Lactate dehydrogenase (LDH) release assay

To assess cellular toxicity induced by LPS, a release assay for LDH was conducted. Chondrocytes were meticulously plated in 96-well plates, exposed to LPS at 1 μg/ml, and incubated for 24 h in a controlled environment with 5 % CO2 at 37 °C. Following the incubation period, varying concentrations of Sip, ranging from 10 to 50 μM, were introduced. The extracellular milieu from the cell cultures was meticulously harvested, and LDH activity was quantified following prescribed protocols (Beyotime, Nanjing, China).

2.9. Real-time PCR (RT-PCR)

Following exposure to 1 μg/ml LPS and Sip at concentrations of 25 or 50 μM, mouse chondrocytes underwent total RNA extraction using TRIzol reagent (Invitrogen). Following reverse transcription to obtain approximately 1000 ng of cDNA, a quantitative real-time polymerase chain reaction (qRT-PCR) was conducted to evaluate the expression of

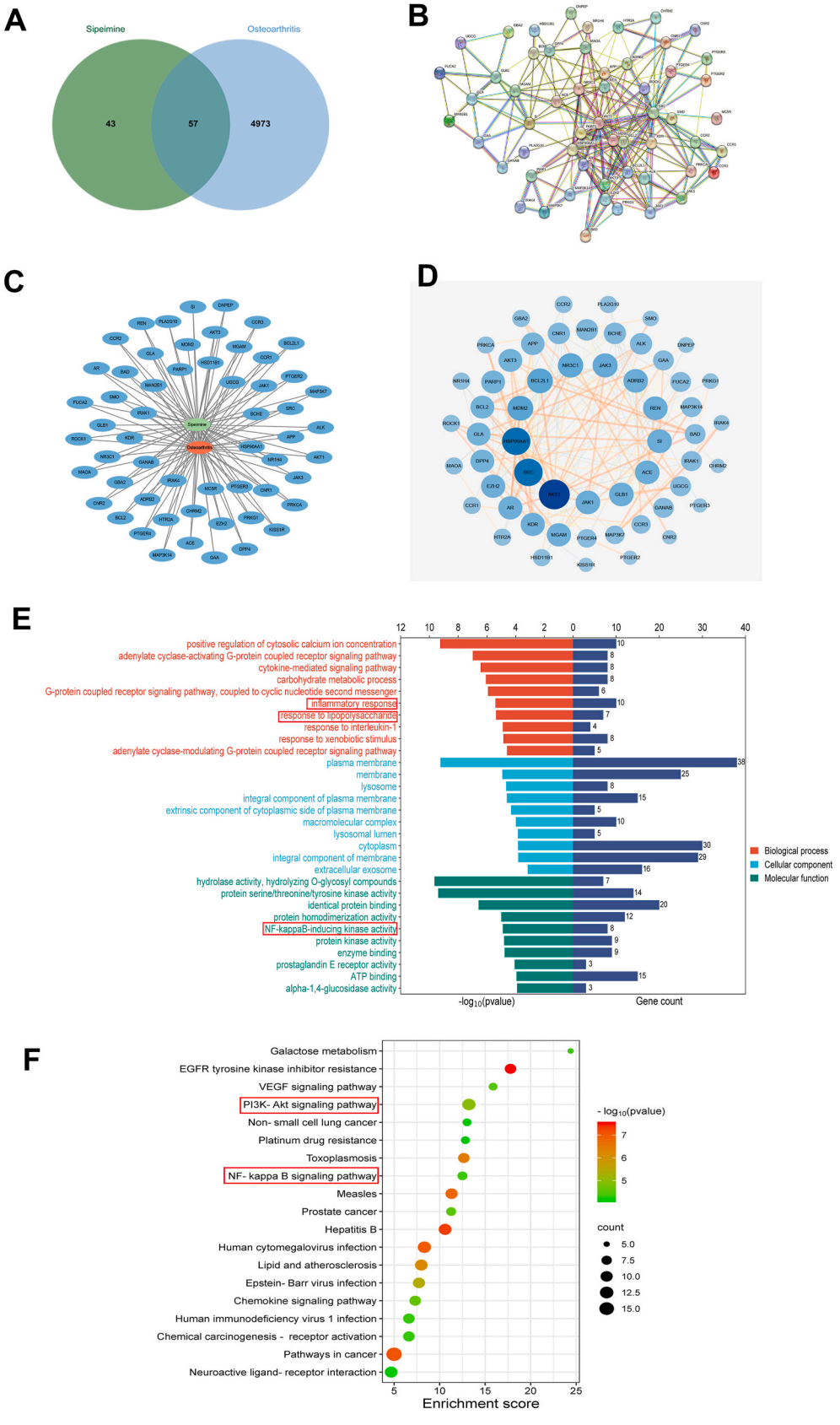

Figure 1. Network pharmacology analysis. (A) Venn diagrams of Sip targets and OA targets. (B) The PPI network of key therapeutic targets. Edges for the association between target genes; nodes for target genes; the more edges connected to the nodes, the higher the degree of the nodes, and these nodes may be at the core of the network. (C) The network of drug-target-disease was constructed. (D) The crucial protein interaction network diagram. The larger the degree of the node in the graph, the darker the colour and the larger the diameter of the node. (E) GO functional annotation for potential targets of Sip on OA. (F) KEGG enrichment analysis for potential targets of Sip on OA. (For interpretation of the references to colour in this figure legend, the reader is referred to the Web version of this article.)

COX-2, iNOS, IL-18, and IL-1β genes. Using the ΔΔCT method, the analysis was conducted with GAPDH as the reference gene [27]. The primer sequences for the target genes were shown in Table 1.

2.10. Western blotting

After assessing cell viability, chondrocytes underwent a 2h pre-exposure phase with varying concentrations of Sip, followed by the application of LPS (1 μg/ml) for an additional 2 h. After treatment, chondrocytes were collected, washed with prechilled PBS, and subsequently lysed using ice-cold RIPA lysis buffer that included a 1 % proteinase inhibitor cocktail from Beyotime. After a 10-min preparation of lysates, a 15-min centrifugation at 12,000 rpm was carried out at 4 °C, followed by quantifying the protein concentration in the samples using the Beyotime BCA protein assay kit. Following that, 25 μg of protein samples were meticulously segregated and transferred onto 12 % SDS-PAGE gels, subsequently translocating them onto polyvinylidene fluoride membranes. Blocking for 2 h was carried out using 5 % skimmed milk. Before an overnight incubation at 4 °C with specified primary antibodies, including NLRP3 (1: 1000), COX-2 (1: 1000), iNOS (1: 1000), Lamin B (1: 1000), cleaved-caspase-1 (1:1000), caspase-1 (1:1000), GAPDH (1:5000), MMP-13 (1: 1000), collagen-II (1: 1000), GSDMD (1:1000), cle-GSDMD (1:1000), aggrecan (1: 1000), ADAMTS-5 (1: 1000), p-p65 (1: 1000), p65 (1: 1000), p-ikBα (1: 5000), ikBα (1: 5000), p-AKT (1:500), AKT (1:1000), p-PI3K (1:1000), PI3K (1:1000), and ASC (1:1000). Following a 2h incubation at room temperature with the suitable secondary antibody, the membranes underwent three washes with TBST. Subsequently, blots were visualized through electrochemiluminescence and an Invitrogen reagent. The measurement of blot intensity was then carried out utilizing Image Lab 3.0 software from Bio-Rad.

2.11. Immunofluorescence microscopy

Immunofluorescence was employed to assess collagen-II, MMP-13, NLRP3, and p65 levels and their distribution within chondrocytes in vitro after different treatments. Initially, cells underwent PBS washing and a 15-min fixation in 4 % paraformaldehyde. Subsequently, cellular permeabilization was achieved with a 15-min incubation in 0.1 % Triton X-100. For an hour, a blocking solution of 5 % Bovine Serum Albumin (BSA) in PBS was employed to establish an optimal experimental environment. Primary antibodies targeting MMP-13, collagen-II, NLRP3, and p65 were applied to chondrocytes for a 12h incubation at 4 °C with a dilution of 1:50. Subsequently, chondrocytes were subjected to a 1h incubation in darkness with a carefully introduced fluorescein-conjugated secondary antibody, followed by a 1-min staining with DAPI (Beyotime). Detection of the cell samples was conducted using an Olympus fluorescent microscope (Tokyo, Japan). The fluorescence intensity was measured using Image J software.

2.12. Radiographic and microcomputed tomography analysis

After an 8-week recovery period post-surgery, mice were euthanized in a humane manner, and their knee joints were gathered and fixed overnight in 4 % paraformaldehyde. Subsequently, every group underwent X-ray and micro-computed tomography (μCT) examinations to evaluate knee joint degradation, encompassing arthrostenosis, joint surface condition, and osteophyte formation. The Faxitron X-ray imaging cabinet (Faxitron Bioptics, Tucson, AZ) was utilized for radiographic analysis. The SkyScan-1276 micro-computed tomography (μCT) system (Bruker micro-CT, Belgium) was then employed for knee joint scans and in-depth assessment, enabling a comprehensive evaluation of knee joint health based on three-dimensional structural parameters.

2.13. Histopathological analysis

At the culmination of the 8-week postoperative period, joint samples were procured from mice by excising the associated tissues, and they were preserved for 48 h in a 4 % paraformaldehyde solution. Following the collection of joints, a 10 % ethylenediaminetetraacetic acid (EDTA) solution was employed for decalcification at 4 °C over one month using a shaker. Following these initial steps, the tissues underwent a series of procedures, encompassing dehydration, paraffin embedding, and sectioning into 5 μm thick slices. Morphological analysis and quantification were then carried out using Safranin O-fast green (S–O) and Hematoxylin-Eosin (H-E) staining. The widely recognized International Osteoarthritis Research Society (OARSI) scoring system, which assigns scores ranging from 0 to 12, was employed to assess the extent of cartilage degeneration. For evaluating synovitis severity, a well-established scoring system, as described in prior research was utilized [28].

2.14. Immunohistochemical staining

Deparaffinization and ethanol gradient-based hydration were applied to mouse knee joint sections. Subsequently, histological sections underwent a 30-min treatment at 37 °C with hydrogen peroxide (3 % v/v) and trypsin–EDTA solution (0.25 %). Following this, a 30-min blocking phase with the application of 10 % donkey serum at 37 °C was initiated. Primary antibodies targeting specific interests, including MMP-13, collagen-II, NLRP3, and P-PI3K, were diluted to a concentration of 1:200 and incubated overnight at 4 °C. Following this, tissue sections underwent a sequential incubation step with a secondary antibody conjugated with horseradish peroxidase (HRP) for 1 h at 37 °C. Utilizing Image-Pro Plus version 6.0 (Media Cybernetics, MD, USA), image and quantitative analyses were conducted on three distinct portions representing diverse groups.

2.15. Statistical analysis

The SPSS program (Chicago, IL, USA) was employed for data analysis, utilizing the unpaired two-tailed Student's t-test or the Chi-square test to assess statistical differences between groups, applying single-factor analysis of variance (ANOVA) for multi-group comparisons, and utilizing the Kruskal–Wallis H test for non-parametric data. The significance threshold was established at $p < 0.05$. Each experiment was replicated three times independently.

3. Results

3.1. Network pharmacology analysis

Determining the chemical structure formula of Sip was accomplished through the SwissTarget Prediction database, unveiling a total of 100 target genes interactions. Subsequent exploration through the GeneCard database unveiled 5030 target genes associated with OA. The co-identification of 57 genes shared between Sip and OA is presented in Fig. 1A. Utilizing the STRING database, a Protein–Protein Interaction (PPI) network was constructed based on these genes (Fig. 1B). Importing data from the STRING database, Cytoscape software (version 3.6.2) was utilized to create both the protein interaction network and the network diagram for Sip-target-disease. Arranged according to their degree values, the target genes were depicted in the network diagram, as illustrated in Fig. 1C and D. GO enrichment analysis demonstrated a robust correlation between Sip and various biological processes (BP) associated with OA, such as inflammatory response and response to LPS; molecular function (MF), including the NF-κB-inducing kinase activity (Fig. 1E). The KEGG enrichment analysis results emphasized the pivotal roles of the NF-κB and PI3K-AKT signaling pathways in the potential treatment of OA with Sip (Fig. 1F).

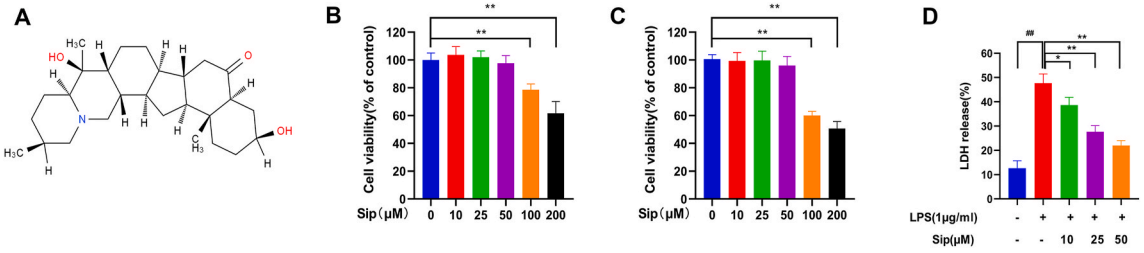

Figure 2. Effect of Sip on mouse chondrocytes viability. (A) Chemical structure of Sip. (B, C) The cytotoxic effect of Sip was detected at different concentrations (0, 10, 25, 50, 100, 200 μM) using the CCK-8 assay after 24 and 48 h of treatment administration. (D) LDH release assays were conducted to measure LPS-induced cytotoxicity. Data are presented as means ± SD, $^{\#\#}p < 0.01$ versus the control group; *p < 0.05; **p < 0.01 versus the LPS-only treatment group; n = 3.

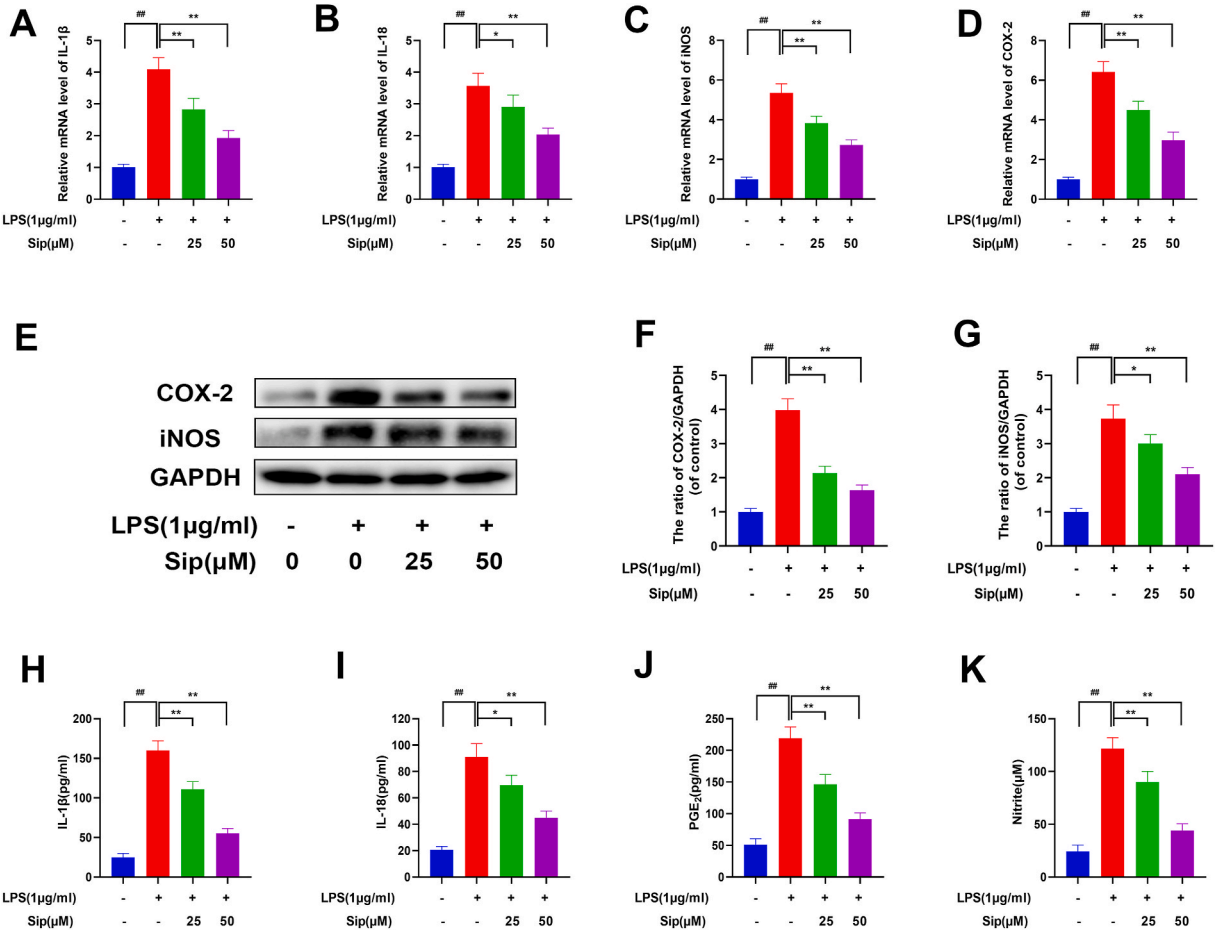

Figure 3. Effect of Sip on LPS-induced inflammation in mouse chondrocytes. The chondrocytes were seeded in the culture dish for 24 h and then exposed to LPS (1 μg/ml) with or without Sip (25, 50 μM) for additional 24 h. (A–D) Real-time PCR for the effects of Sip on mRNAs levels of IL-1β, IL-18, iNOS and COX-2 in chondrocytes. The expression levels of these genes were normalized to the expression of GAPDH. (E–G) Western blot analysis for the effects of Sip on iNOS and COX-2 protein levels in chondrocytes. (H–K) ELISA test for the effects of Sip on IL-1β, IL-18, nitrite and PGE_2 levels in the cell culture supernatants after indicated treatment. Data are presented as means ± SD, $^{\#\#}p < 0.01$ versus the control group; *p < 0.05; **p < 0.01 versus the LPS-only treatment group; n = 3..

3.2. Effect of Sip on mouse chondrocytes viability

Fig. 2A presents the chemical molecular structure of Sip. The evaluation of chondrocyte toxicity induced by Sip employed CCK-8 at specified concentrations (0, 10, 25, 50, 100, and 200 μM). The results revealed a noteworthy decrease in chondrocyte vitality at 100 and 200 μM after 24 and 48 h (Fig. 2B and C). In assessing LPS-induced cytotoxicity, we conducted LDH release assays. LPS stimulation prompted an elevation in LDH levels, while Sip intervention demonstrated a dose-responsive inhibition of LPS-induced LDH release (Fig. 2D).

3.3. Effect of Sip on LPS-induced inflammation in mouse chondrocytes

The study employed a combination of qRT-PCR, western blot, and ELISA techniques to precisely detect protein and mRNA levels of inflammatory markers within the chondrocytes. The results from both PCR and ELISA revealed a significant elevation in IL-1β, IL-18, PGE2 and nitrite levels following LPS administration. Sip treatment effectively suppressed these heightened levels, as demonstrated in Fig. 3A and B and Fig. 3H–K. Moreover, the results revealed a dose-dependent alleviation by Sip treatment in chondrocytes, effectively reducing the heightened levels of COX-2 and iNOS induced by LPS treatment. This

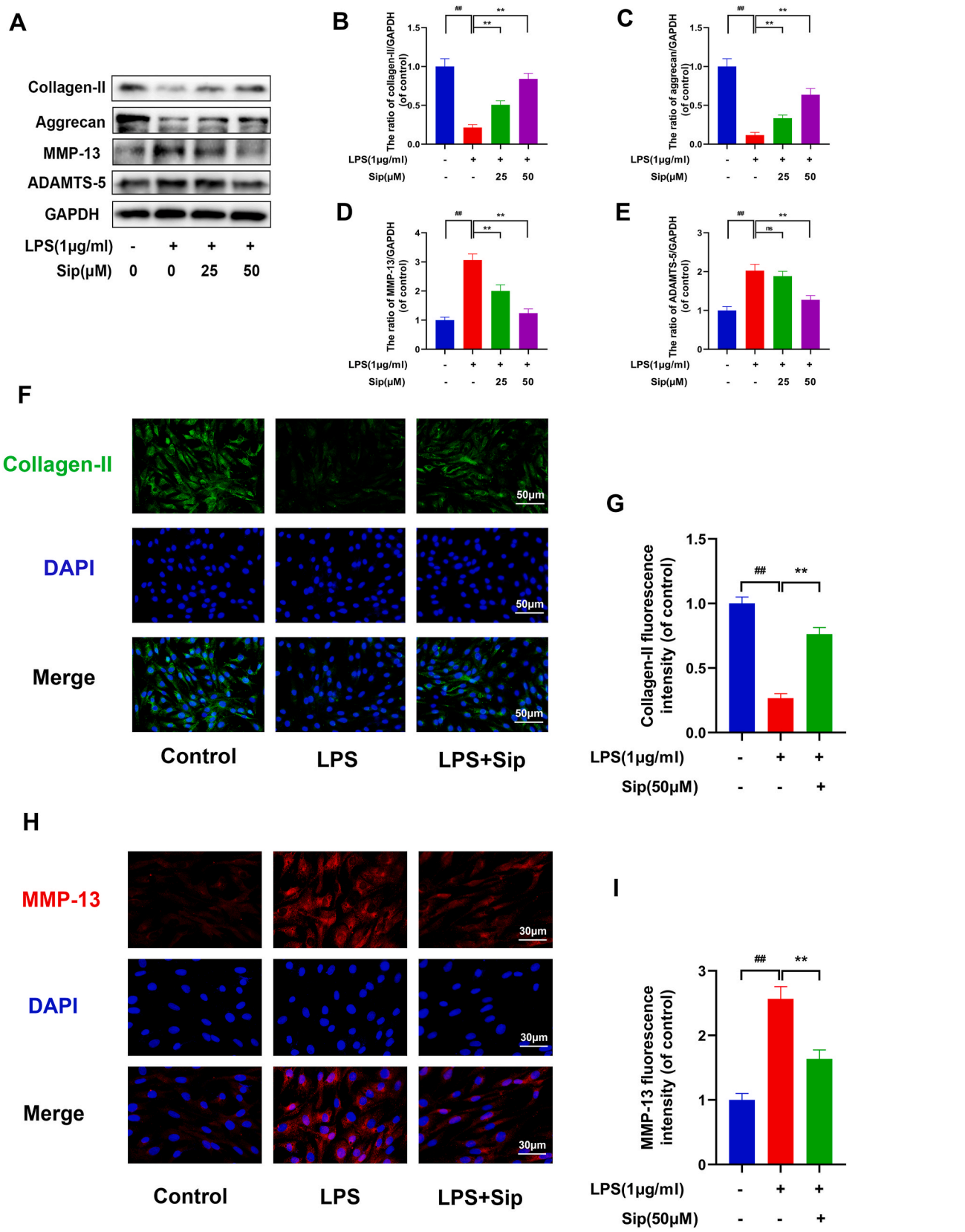

Figure 4. Sip suppresses ECM degradation in LPS-induced mouse chondrocytes. The chondrocytes were seeded in the culture dish for 24 h and then exposed to LPS (1 μg/ml) with or without Sip (25, 50 μM) for additional 24 h. (A–E) Western blot analysis for the effects of Sip on collagen-II, aggrecan, MMP-13 and ADAMTS-5 protein levels in chondrocytes. (F–I) Immunofluorescence staining and quantitative analysis of collagen II and MMP-13 in chondrocytes treated with LPS (1 μg/ml) in the presence or absence of Sip (50 μM) for 24 h. Data are presented as means ± SD, $^{\#\#}p < 0.01$ versus the control group; $^{*}p < 0.05$; $^{**}p < 0.01$ versus the LPS-only treatment group; n = 3.

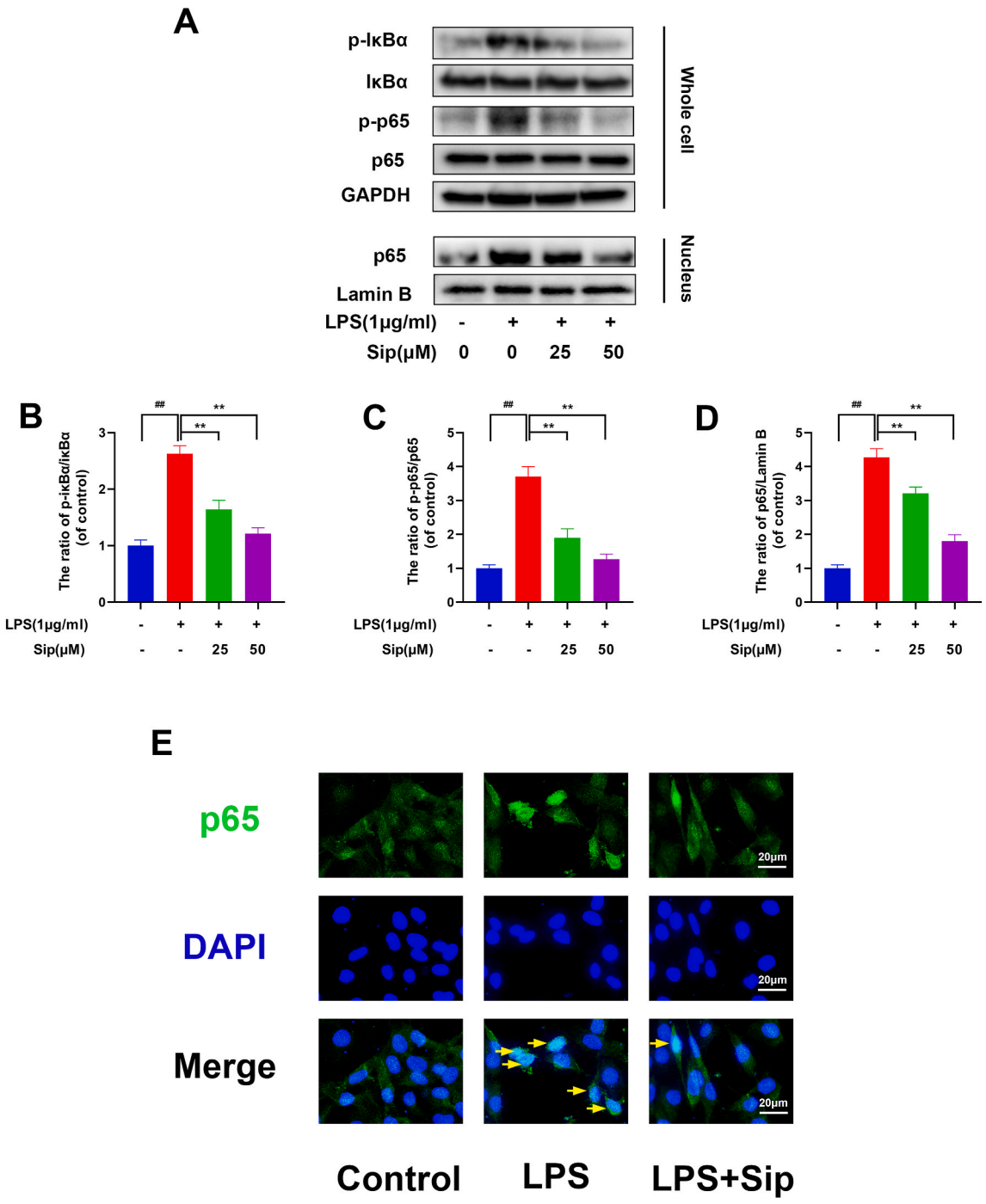

Figure 5. Sip inhibits LPS-induced NF-κB pathway activation in mouse chondrocytes. The chondrocytes were exposed to Sip (50 μM) for 2h followed with LPS (1 μg/ml) for additional 2 h. (A–D) Effect of Sip on the expression of IκBα and p65 as well as their phosphorylation in the whole cell and p65 expression in the nucleus as determined by western blotting. (E) The effect of Sip on p65 translocation to the nucleus as detected through immunofluorescence assay in chondrocytes treated with Sip (50 μM) for 2 h followed with LPS (1 μg/ml) for additional 2 h (yellow arrows showed the p65 translocation to the nucleus). Data are presented as means ± SD, $^{\#\#}p < 0.01$ versus the control group; $^{*}p < 0.05$; $^{**}p < 0.01$ versus the LPS-only treatment group; n = 3. (For interpretation of the references to colour in this figure legend, the reader is referred to the Web version of this article.)

effect was evident at both the protein and mRNA levels, as depicted in Fig. 3C–G.

3.4. Sip suppresses ECM degradation in LPS-induced mouse chondrocytes

We systematically evaluated the expressions of collagen-II, aggrecan, MMP-13 and ADAMTS-5 to investigate the impact of Sip on LPS-induced ECM degradation in mouse chondrocytes. The results from protein blots demonstrated that, in a dose-dependent manner, Sip increased aggrecan and collagen-II levels while suppressing MMP-13 and ADAMTS-5 in chondrocytes exposed to LPS stimulation (Fig. 4A–E). Furthermore, the outcomes of cell immunofluorescence and quantitative analysis of MMP-13 and collagen-II aligned with the previously mentioned findings, thus validating Sip's protective influence on chondrocyte ECM integrity (Fig. 4F–I).

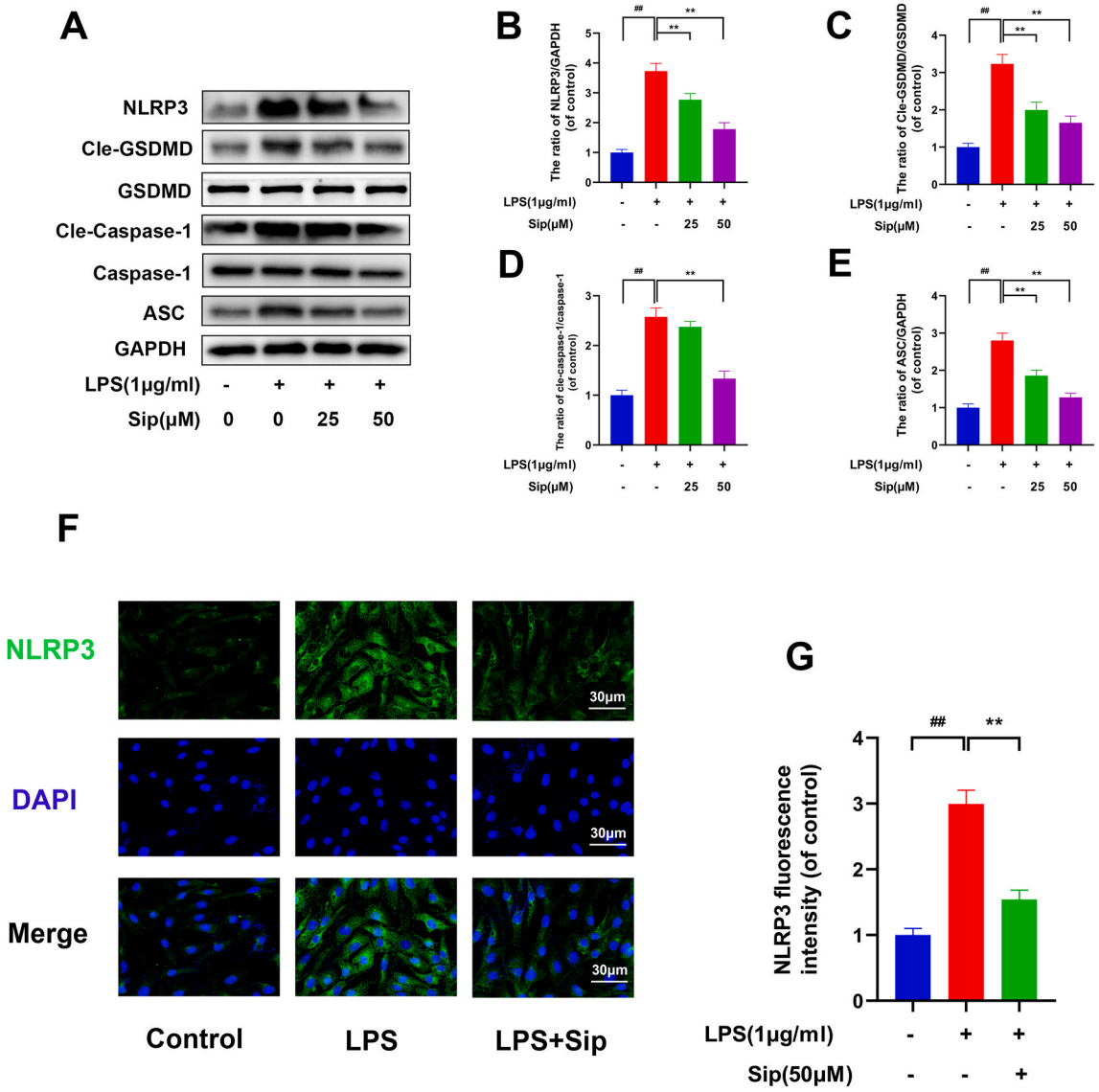

Figure 6. Sip inhibits LPS-induced NLRP3 inflammasome activation and pyroptosis in mouse chondrocytes. The chondrocytes were seeded in the culture dish for 24 h and then exposed to LPS (1 μg/ml) with or without Sip (25, 50 μM) for additional 24 h. (A–E) Western blot analysis for the effects of Sip on NLRP3, cle-GSDMD, cle-caspase-1 and ASC protein levels in chondrocytes. (F–G) Immunofluorescence staining and quantitative analysis of NLRP3 in chondrocytes treated with LPS (1 μg/ml) in the presence or absence of Sip (50 μM) for 24 h. Data are presented as means ± SD, $^{\#\#}p < 0.01$ versus the control group; $^{*}p < 0.05$; $^{**}p < 0.01$ versus the LPS-only treatment group; n = 3.

3.5. Sip inhibits LPS-induced NF-κB pathway activation in mouse chondrocytes

We conducted an examination of the influence of Sip on NF-κB levels subsequent to LPS treatment with the objective of elucidating the mechanism through which Sip mitigates inflammation and ECM degradation. LPS application induced p65 and IκB-α phosphorylation in the whole cell, culminating p65 translocation into the nucleus, ultimately fostering inflammatory factor production. Through Western blot analysis, we observed that Sip treatment mitigated this process by diminishing the phosphorylation of IκB-α and p65, concurrently suppressing nuclear p65 expression (Fig. 5A–D). Simultaneously, immunofluorescence experiments validated the observation that LPS induced the translocation of p65 from the cytoplasm to the nucleus. Conversely, Sip demonstrated the capacity to inhibit p65's nuclear translocation (Fig. 5E).

3.6. Sip inhibits LPS-induced NLRP3 inflammasome activation and pyroptosis in mouse chondrocytes

We conducted protein blotting experiments to explore Sip's influence on NLRP3 inflammasome activation and pyroptosis after LPS treatment. The result of Western blot analysis showed that NLRP3, cle-GSDMD, cle-caspase-1 and ASC were significantly up-regulated after treatment with LPS. However, Sip negatively regulated LPS-induced NLRP3 inflammasome activation and pyroptosis-related markers (Fig. 6A–E). Immunofluorescence assessment of NLRP3 expression supported the protein blotting findings (Fig. 6F and G). Consequently, Sip's inhibitory action effectively alleviated chondrocyte pyroptosis.

3.7. Sip protects chondrocytes from pyroptosis by inhibiting PI3K/AKT/NF-κB signaling pathway

Various investigations have underscored the noteworthy characteristics of Sip, demonstrating its effectiveness in mitigating inflammation

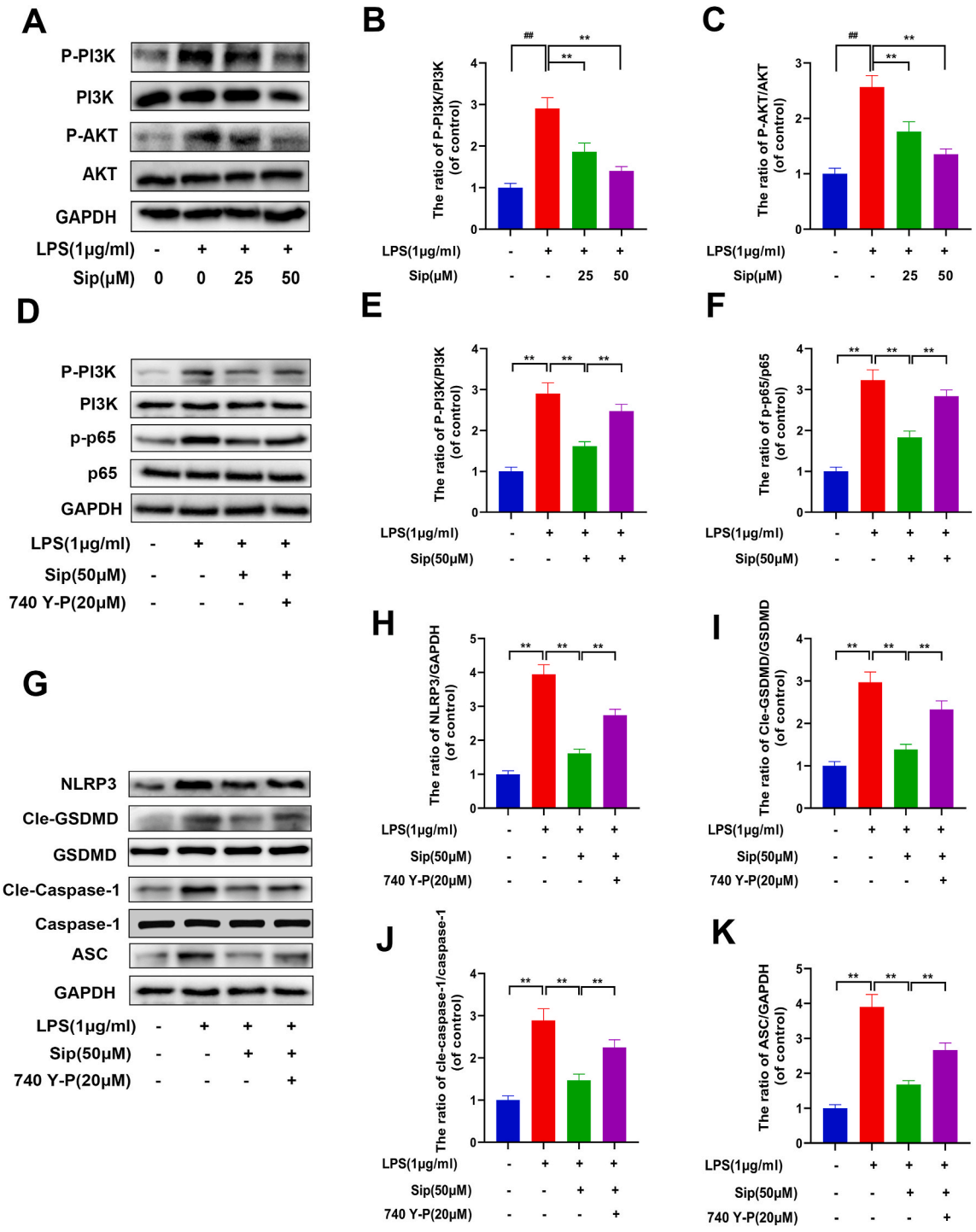

Figure 7. Sip protects chondrocytes from pyroptosis by inhibiting PI3K/AKT/NF-κB signaling pathway. (A–C) The chondrocytes were exposed to Sip (50 μM) for 2 h and then to LPS (1 μg/ml) for additional 2 h. Effect of Sip on the expression of PI3K and AKT as well as their phosphorylation as determined by western blotting. (D–F) After treatment with 740 Y–P(20 μM) for 2 h, the chondrocytes were exposed to Sip (50 μM) for 2 h followed by LPS (1 μg/ml) for additional 24 h. Western blotting results revealing the effects of Sip on expression levels of PI3K and p65 as well as their phosphorylated forms after 740 Y–P treatment.(G–K) Western blotting results showing expression of NLRP3, cle-GSDMD, cle-caspase-1 and ASC in chondrocytes treated with 740 Y–P and subsequently treated with LPS (1 μg/ml) in the presence or absence of Sip (50 μM) for 24 h. Data are presented as means ± SD, *p < 0.05; **p < 0.01; n = 3.

by inhibiting the PI3K/AKT/NF-κB signaling pathway. Using western blotting, we evaluated alterations in the expression of PI3K/AKT/NF-κB pathway components, measuring levels of PI3K, AKT and p65 along with their phosphorylated forms. The induction of LPS resulted in a notable increase in the phosphorylation levels of AKT and PI3K in comparison to the control group. Whereas, Sip effectively mitigated these changes (Fig. 7A–C). For a comprehensive investigation into the specific role of the PI3K/AKT pathway in the anti-inflammatory and chondroprotective effects of Sip, we utilized 740 Y–P (a PI3K activator) to induce PI3K activation. The Western blot analysis results demonstrated a significant attenuation by 740 Y–P of the inhibitory effects induced by Sip on PI3K and p65 phosphorylation (Fig. 7D–F). Furthermore, 740 Y–P nullified Sip's inhibitory effect on NLRP3-mediated chondrocyte pyroptosis (Fig. 7G–K). Similarly, activating PI3K by 740 Y–P reversed the

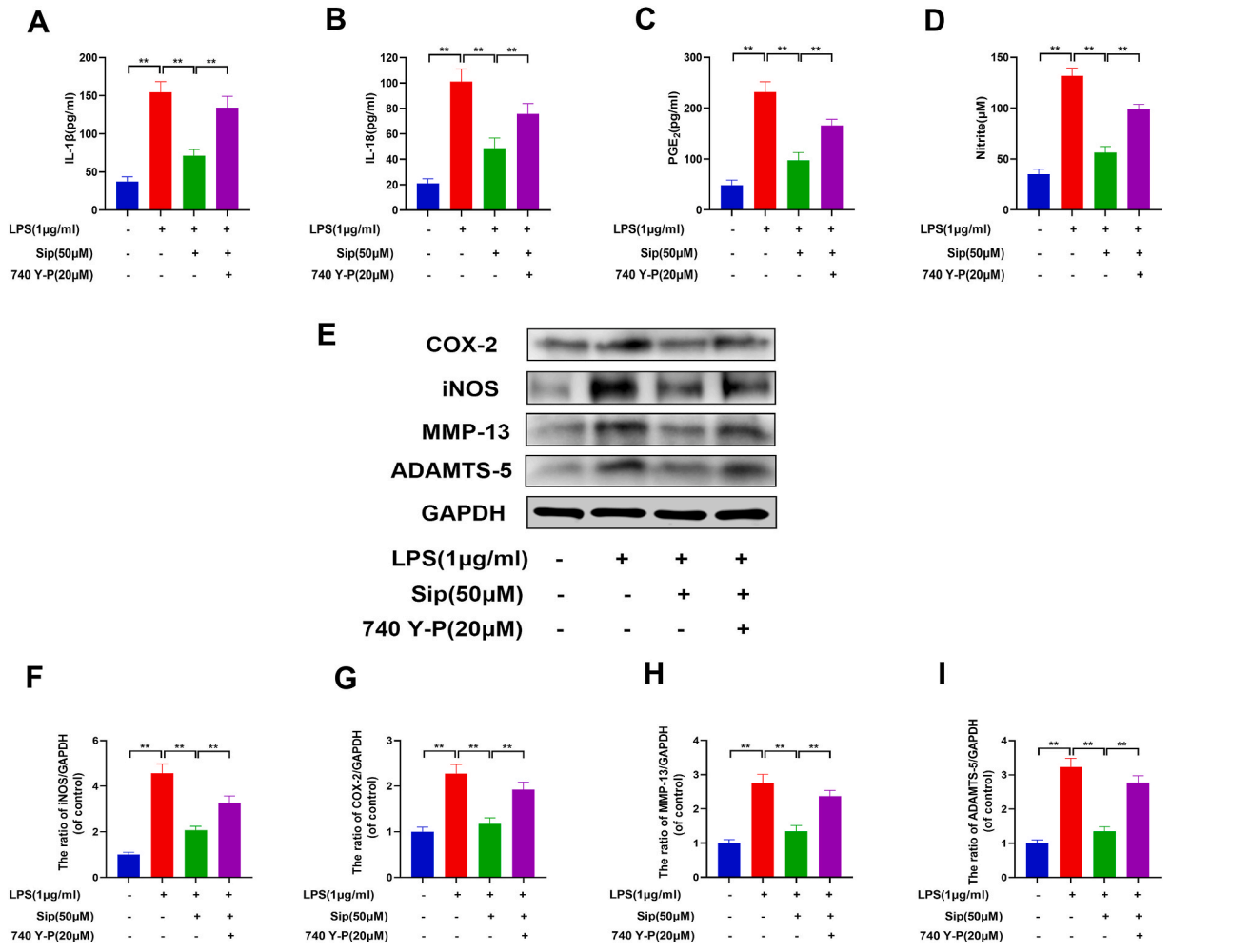

Figure 8. Sip exerts protective effects against inflammation and ECM degradation via suppressing PI3K/AKT/NF-κB signaling pathway. (A–D) ELISA results showing expression of IL-1β, IL-18, nitrite and PGE_2 levels in chondrocytes treated with 740 Y–P and subsequently treated with LPS (1 μg/ml) in the presence or absence of Sip (50 μM) for 24 h. (E–I) Western blotting results showing expression of COX-2, iNOS, MMP-13 and ADAMTS-5 in chondrocytes treated with 740 Y–P and subsequently treated with LPS (1 μg/ml) in the presence or absence of Sip (50 μM) for 24 h. Data are presented as means ± SD, *p < 0.05; **p < 0.01; n = 3.

suppressive effects of inflammatory factors and ECM degradation caused by Sip in chondrocytes (Fig. 8A–I). Consequently, Sip exerts protective effects against NLRP3-mediated pyroptosis, ECM degradation and inflammation through inhibiting the signaling pathway of PI3K/AKT/NF-κB.

3.8. Molecular docking

Consistent with the results of the molecular docking assessment, Sip demonstrated a strong binding affinity for both PI3K and p65, with binding energy values of −8.9 kcal/mol and −9.4 kcal/mol, respectively. This suggests the stable formation of complexes between Sip and both p65 and PI3K. 3D structural modeling depicted the integration of the Sip molecule into the binding pockets of p65 and PI3K (Fig. 9A and D). Regarding p65, hydrogen bonds were established with the ASN-274 residue by Sip (Fig. 9B). Similarly, Sip formed hydrogen bonds with the GLU-926 and GLU-209 residues of PI3K, as observed in Fig. 9E. Hydrophobic interactions were found between the Sip molecule and p65's HIS-137 residue as well as PI3K's TYR-930 residue (Fig. 9C and F). The findings revealed that PI3K/AKT/NF-κB signaling was implicated in Sip's protective effects in OA.

3.9. Sip alleviates the progression of osteoarthritis in a mouse model

In order to evaluate the potential therapeutic impact of Sip on osteoarthritis (OA) in mice, we assigned mice randomly to three groups: a sham surgery group, a DMM group, and a DMM + Sip (30 mg/kg) group. Using X-ray and Micro-CT 3D reconstruction techniques, we observed that the DMM group mice exhibited characteristic osteoarthritic features, including joint space narrowing and osteophyte formation. Mice subjected to Sip treatment exhibited a notably expanded joint space, more even joint surfaces, and a decreased count of osteophytes in comparison to the DMM group, as illustrated in Fig. 10A and B. The quantitative analysis disclosed a significant decrease in subchondral bone volume/tissue volume (BV/TV), trabecular thickness (Tb.Th), and trabecular number (Tb.N), alongside an elevation in trabecular separation (Tb.Sp) within the DMM group relative to the sham surgery group, along with a notably increased count of osteophytes (Fig. 10C–G). However, Sip showed a slight improvement in subchondral remodeling, resulting in more smoother and intact bone structures (Fig. 10C–G). Additionally, we performed HE and SO staining procedures to appraise the condition of the articular cartilage tissue and synovium. In comparison to the sham group, the DMM group experienced a significant rise in OARSI scores, while the DMM + Sip group demonstrated markedly lower scores than the DMM group (Fig. 11A and B). Furthermore, Sip treatment resulted in a significant reduction in synovitis compared to the DMM group (Fig. 11A and C). Immunohistochemistry results demonstrated an overexpression of MMP-13, NLRP3 and P-PI3K as well as lower expression of collagen-II in the DMM group. Sip treatment significantly reduced MMP-13, NLRP3 and P-PI3K expression and

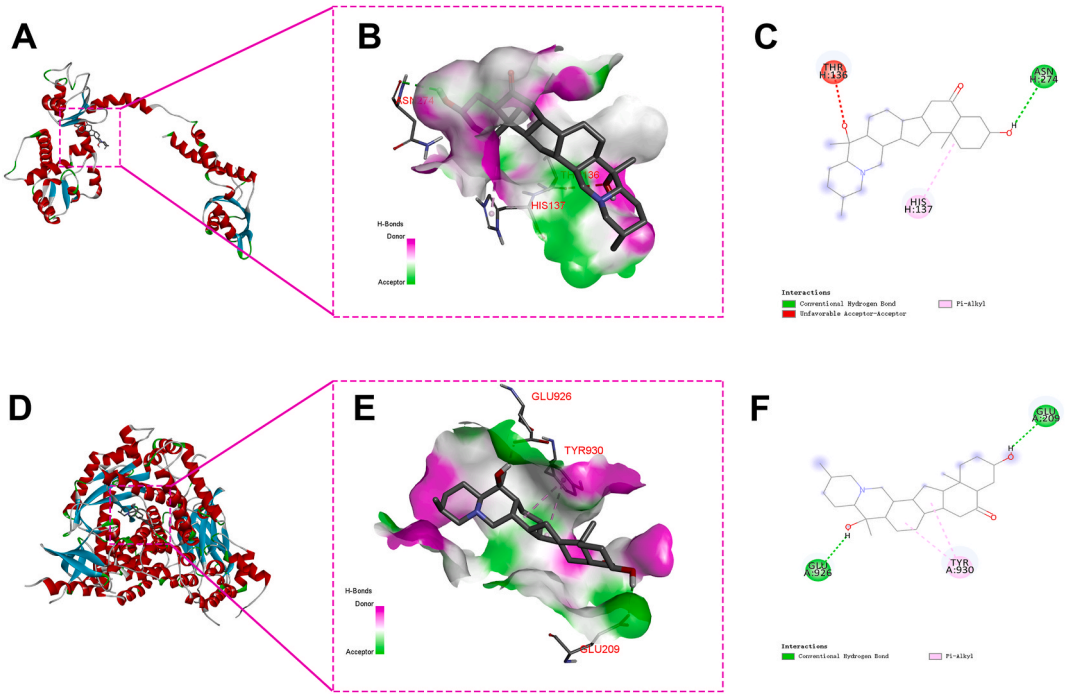

Figure 9. Molecular docking of Sip on its p65 and PI3K binding site. (A and D)3D structural modeling results showed that the Sip molecule was enclosed within the binding pockets of p65 and PI3K.(B and E) Hydrogen bonds between Sip and neighboring amino acid residues in p65 and PI3K.(C and F) Hydrophobic interactions interactions between Sip and p65 and PI3K at the binding site..

increased collagen-II expression (Fig. 11D–H). In summary, these collective findings indicate that Sip treatment effectively safeguards knee joint tissues from damage and mitigates the progression of OA.

4. Discussion

OA is a complex degenerative joint disorder marked by the gradual erosion of cartilage within the joint structures [29]. Its development is influenced by a myriad of physiological and pathological factors [30]. The primary approach to treatment relies on non-steroidal anti-inflammatory drugs to manage pain [31]. Consequently, the quest for novel therapeutics capable of effectively impeding cartilage degeneration in osteoarthritic joints is of paramount significance. Sip is a naturally occurring bioactive compound derived from *Fritillariae Cirrhosae Bulbus* [32]. Until now, the potential therapeutic effects of Sip on OA have not been explored, despite comprehensive examinations of its diverse medicinal properties in both in vitro and in vivo settings. This investigation combines network pharmacology, molecular docking, and in vitro as well as in vivo experiments to elucidate Sip's potential impact on murine OA.

Inflammation stands as a fundamental facet in OA pathogenesis, with its pivotal role well-established [33]. During OA progression, chondrocytes produce notable inflammatory cytokines, such as IL-6, IL-18, and NO [34]. It has been established that inflammation drives various pathological changes within the context of OA, exacerbating joint cartilage deterioration [35]. In this study, we have unveiled Sip's capacity to suppress the emergence of inflammation in chondrocytes introduced by LPS, causing inflammatory mediators reduction, such as COX-2, iNOS, nitrite and PGE2. Our results align with prior studies, demonstrating Sip's efficacy in suppressing the synthesis of pro-inflammatory cytokines, such as COX-2, iNOS, NO, and TNF-α, in LPS-stimulated RAW 264.7 macrophages [24]. Moreover, aside from inflammation, the perturbation of ECM metabolism, culminating in ECM degradation, significantly contributes to OA progression [36]. This is evidenced by the downregulation of crucial joint cartilage matrix components like aggrecan and collagen-II, along with an upregulation of degenerative markers like MMPs and ADAMTS [37]. The present study demonstrated that Sip increased collagen-II and aggrecan expression while suppressing MMP-13 and ADAMTS-5 in chondrocytes exposed to LPS stimulation, which suggests that Sip has protective effects in reshaping the joint microenvironment.

Caspase-1 activity within the inflammasome is recognized for inducing cell death in a highly inflammatory process which called pyroptosis [38]. The process entails the activation of caspase-1, leading to the maturation and release of IL-18 and IL-1β, thereby enhancing the inflammatory response [39]. Inhibition of caspase-1 has demonstrated a capacity to decelerate the progression of chronic arthritis [40]. Implicated in the pathogenesis of OA, the NLRP3 inflammasome, a crucial element of pyroptosis, displays elevated protein expression in knee OA patients when compared to the control group [15,41]. GSDMD, a well-explored Gasdermin, plays a role in pyroptosis through caspase-1 cleavage, releasing the N-terminal domain. Subsequently, this process forms a cell membrane pore, facilitating the release of substrates like IL-1β and IL-18 [42,43]. Several studies have shown that inhibition of chondrocyte pyroptosis could ameliorate cartilage damage in OA [44–46]. During this investigation, it was observed that Sip markedly decreased the expression of NLRP3, ASC, cle-GSDMD, and cleaved-caspase-1 proteins induced by LPS in mouse chondrocytes. Collectively, these findings indicate that Sip has the capacity to suppress the NLRP3 inflammasome, thereby attenuating LPS-induced pyroptosis and inhibiting cartilage degradation.

Activation of the NLRP3 inflammasome and initiation of GSDMD-mediated pyroptosis necessitate the engagement of the NF-κB signal transduction pathway, a crucial element for pro-IL-1β expression and a key player in inflammasome initiation and assembly [47]. Regulation of inflammatory mediators through NF-κB signal transduction pathways has been elucidated in prior studies, playing a significant role in the progression of OA [48,49]. Under undisturbed conditions, NF-κB dimers remain localized to the cytoplasm, actively interacting with IκB-α. Upon inflammation stimulation, IκB-α undergoes phosphorylation and subsequent degradation by the proteasome. Phosphorylation of p65 initiates a cascade, ultimately resulting in the translocation of NF-κB

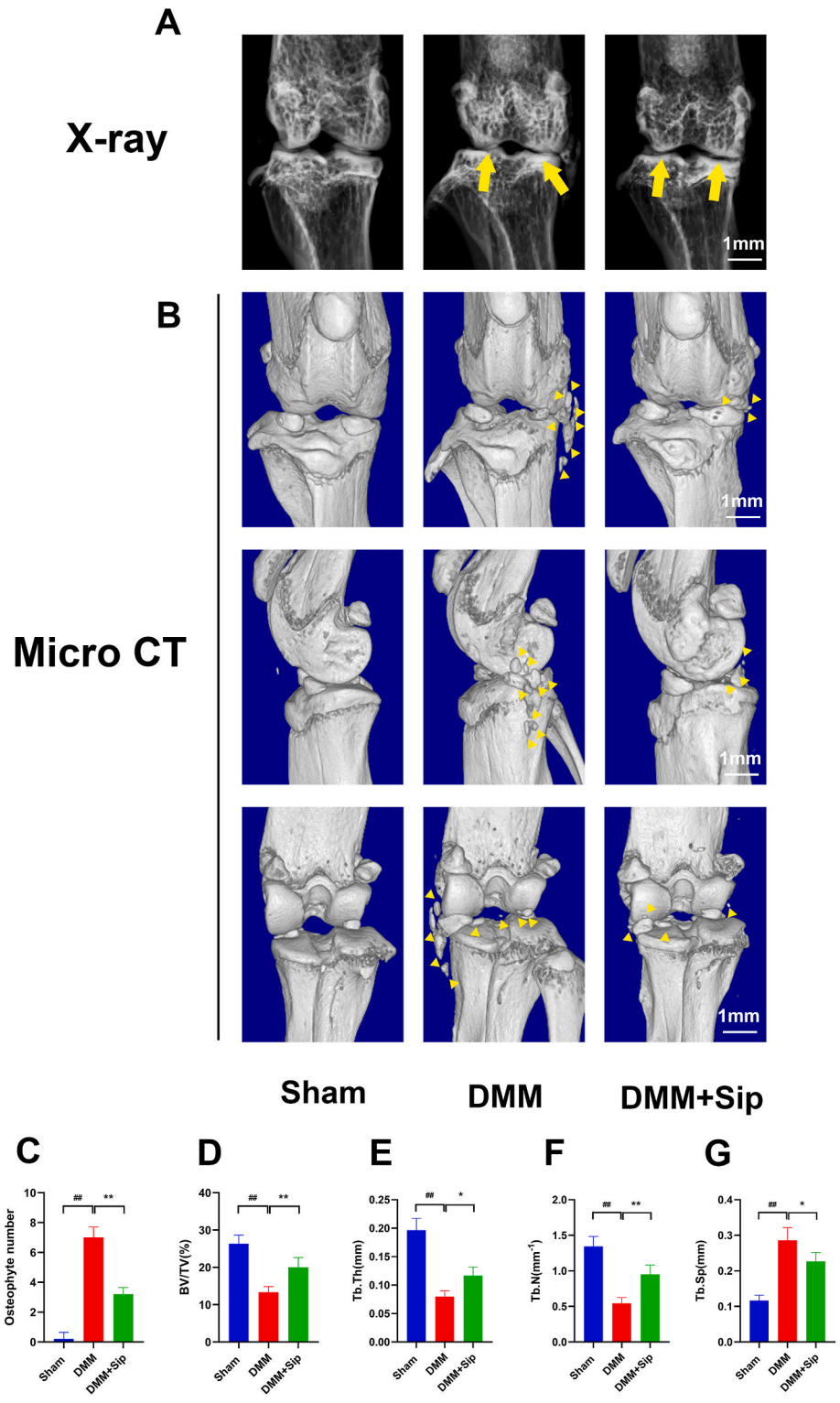

Figure 10. Sip alleviates the changes of subchondral bone in the progression of osteoarthritis in a mouse model. (A) Narrowing of joint spaces was observed in the DMM and Sip treatment groups through X-ray (yellow arrows).(B) 3D reconstruction images of micro-CT scanning of the knees and osteophytes (yellow triangular arrows).(C) The number of osteophytes.(D–G) Quantitative analysis of BV/TV, Tb.Th, Tb.N, and Tb.Sp in subchondral bone. Data are presented as means ± SD, $^{\#\#}p < 0.01$ versus the sham group; $^{**}p < 0.01$ versus the DMM group; n = 15. (For interpretation of the references to colour in this figure legend, the reader is referred to the Web version of this article.)

complexes to the cell nucleus and, consequently, triggering the expression of diverse pro-inflammatory cytokines [50,51]. In the course of this investigation, Sip treatment markedly diminished the phosphorylation of IκB-α and p65, coupled with a reduction in nuclear p65 expression. Concurrently, through inhibiting the nuclear translocation of p65, Sip demonstrated its potential to regulate the NLRP3 inflammasome and pyroptosis by coordinating modulation of NF-κB signaling in mouse chondrocytes.

Employing network pharmacology, we discerned potential targets of Sip against OA. The KEGG analysis revealed that Sip could potentially

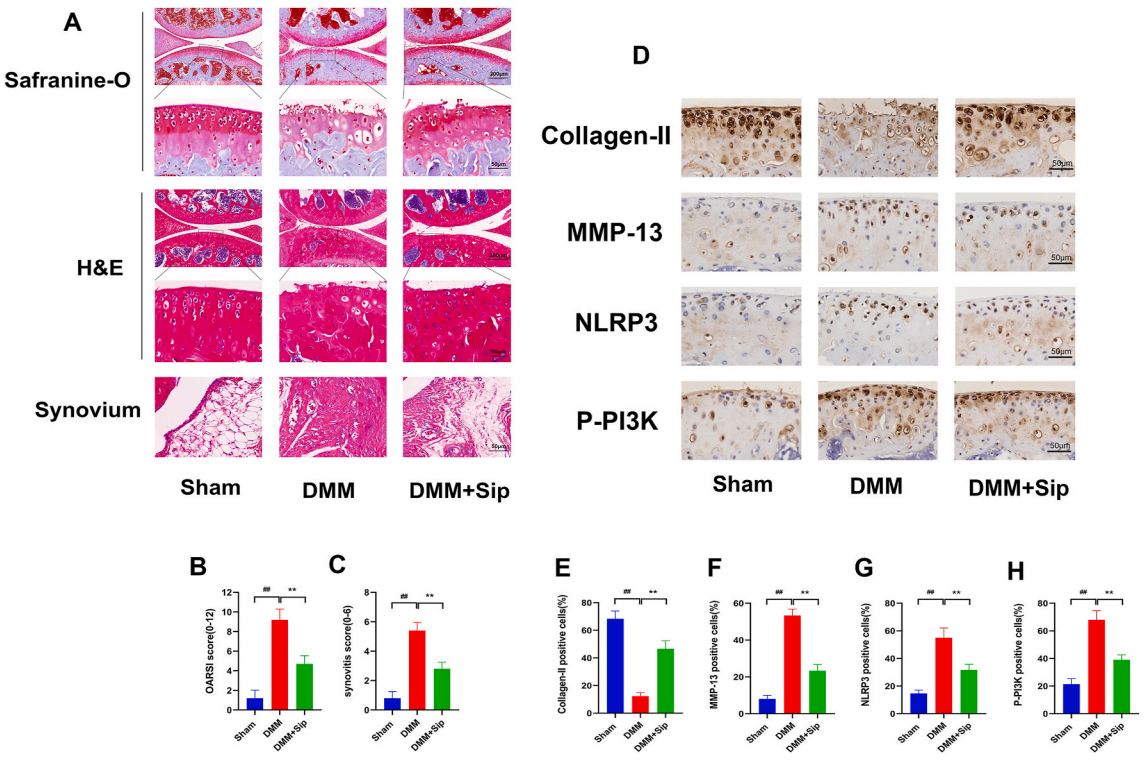

Figure 11. Sip attenuates the staining evaluations in the progression of osteoarthritis in a mouse model. (A) Typical cartilage S–O staining for cartilage and H&E staining for synovium. (B) Cartilage OARSI scores.(C) Synovitis scores.(D–H) Immunohistochemical staining and quantitative analysis for the expression of collagen-II, MMP-13, NLRP3 and P-PI3K in the cartilage tissues. Data are presented as means ± SD, $^{\#\#}p < 0.01$ versus the sham group; $^{**}p < 0.01$ versus the DMM group; n = 15.

confer a protective effect by regulating the signaling pathways of PI3K/AKT and NF-κB. The intracellular PI3K/AKT pathway, linked to ECM alterations in OA pathogenesis [52], undergoes activation upon stimulation, consequently triggering the downstream NF-κB pathway. The subsequent activation induces phosphorylation of IκB-α and p65, ultimately leading to the overexpression of inflammatory mediators in chondrocytes [53]. In our investigation, Sip exerted a significant inhibitory effect on the phosphorylation of PI3K and AKT induced by LPS. To verify the inhibition of the PI3K/AKT signaling pathway by Sip, we employed 740 Y–P (PI3K activator) in our experimental approach. In our findings, 740 Y–P was observed to markedly abolish the suppression of PI3K and p65 phosphorylation induced by Sip, nullifying Sip's inhibitory impact on NLRP3-mediated pyroptosis, inflammatory factor expression, and ECM degradation. Combining network pharmacology analysis with our experimental results, Sip exhibits protective effects against NLRP3-mediated pyroptosis by inhibiting the PI3K/AKT/NF-κB signaling pathway in chondrocytes (Fig. 12). However, our results were not inconsistent with a prior investigation illustrating the mitigating impact of Sip on PM2.5-induced lung toxicity, achieved by suppressing NLRP3 inflammasome-mediated pyroptosis through the activation of the PI3K/AKT pathway [25]. Discrepancies in outcomes may be attributed to differences in diseases, cell types, and animal models used. Consequently, additional research is necessary to elucidate the precise regulatory mechanism of Sip within the realm of OA.

Beyond our in vitro exploration, we conducted an in vivo assessment to investigate the influence of Sip on OA. Numerous animal studies confirm that changes in subchondral bone microarchitecture during the initial phases of OA, corresponding to articular cartilage degeneration [54,55]. Abnormal mechanical loading prompts modeling and remodeling of the subchondral bone, resulting in anomalous restructuring in the early stages of osteoarthritis and the subsequent formation of osteophytes [56]. Our micro-CT analysis reveals that Sip reverses subchondral bone changes in OA, indicating its potential to alleviate OA-related subchondral bone remodeling and reduce osteophyte formation. Additionally, mice in the DMM group exhibited cartilage calcification, erosion, reduced chondrocytes, ECM degradation, and synovitis, as evidenced by HE, S–O, and immunohistochemical staining. Conversely, Sip treatment could mitigate these detrimental effects. Thus, Sip treatment may emerge as a promising therapeutic candidate for OA, as suggested by the combined outcomes of both in vitro and in vivo investigations.

It's important to acknowledge that this study comes with certain limitations. First, we have not explored whether Sip might exert its effects on OA through alternative pathways and mechanisms. Second, the interactions between PI3K/AKT and other pathways have not been investigated. Third, besides the articular chondrocyte, OA involves various cell types, such as synovial fibroblasts, which also undergo changes during OA development. These cellular influences on OA were not considered in this study. As a result, it becomes evident that future research efforts should encompass more comprehensive investigations to further illuminate the therapeutic potential of Sip in the context of OA.

5. Conclusion

In conclusion, the study suggests that Sip mitigates the progression of OA by inhibiting the PI3K/AKT/NF-κB pathway, thereby suppressing NLRP3 inflammasome activation and pyroptosis, and ultimately alleviating both inflammation and ECM degradation. These findings contribute to an enhanced understanding of Sip's potential as a promising therapeutic agent for treating OA.

Credit authors statement

Conception and design of study: Yuqin Fang, Junlei Lv, Chaoyang Zhang; acquisition of data: Ziteng Zhu, Wei Hu; analysis and/or

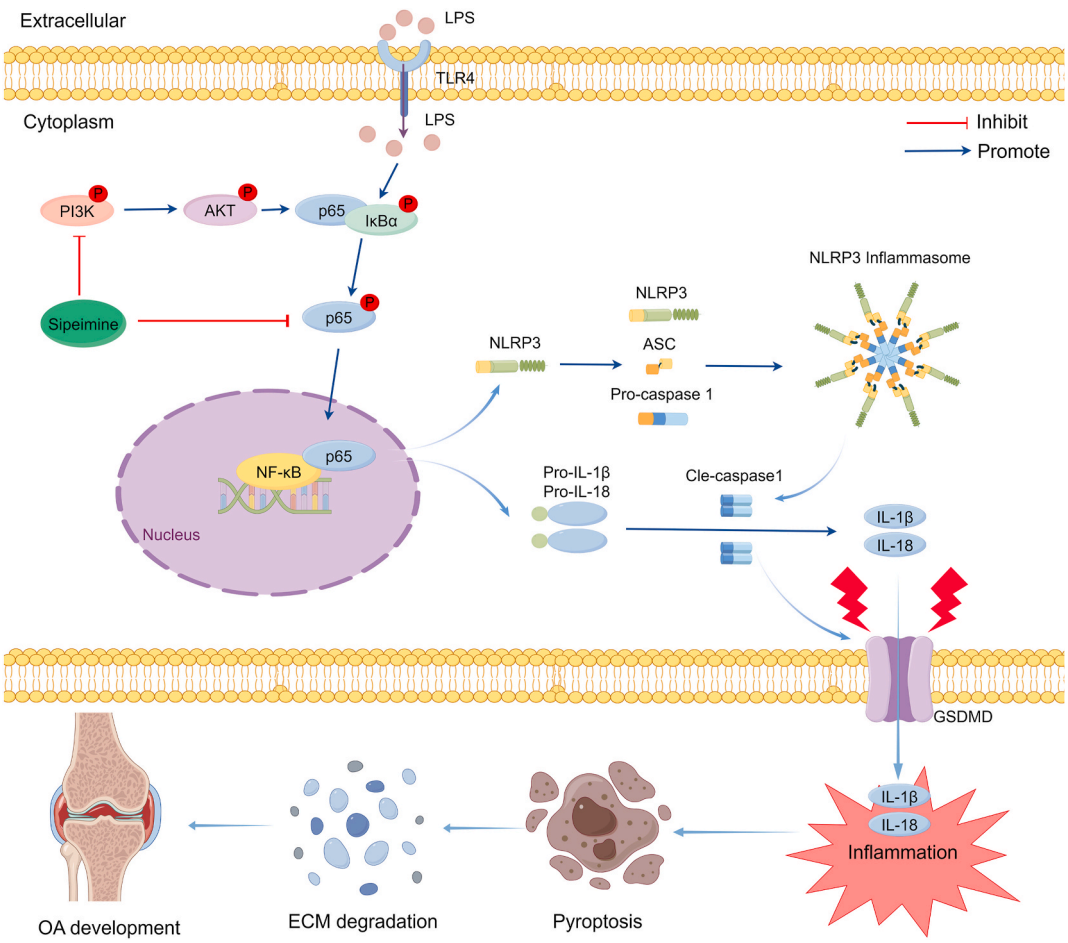

Figure 12. Potential molecular mechanism underlying the protective effects of Sip against osteoarthritis. Sip exerts its protective effects by regulating NLRP3 inflammasome-mediated pyroptosis through suppressing the PI3K/AKT/NF-κB signaling pathway, consequently, alleviating inflammation and ECM degradation to alleviate the progression of OA. (This figure was created by Figdraw)..

interpretation of data: Hua Chen, Liaojun Sun; Drafting the manuscript: Yuqin Fang, Chao Lou, Wenhao Zheng; revising the manuscript critically for important intellectual content: Liaojun Sun, Wenhao Zheng.

Ethics statement

Approval for the ethical treatment and use of experimental animals, adhering to the guidelines stipulated in the National Institutes of Health's Care and Use of Laboratory Animals, was granted by the Animal Care and Use Committee of Wenzhou Medical University (ethic code: wydw2023-0310)

Funding

This work was funded by the Wenzhou Science and Technology Plan Project (Y2023043 and Y20210050), Zhejiang Medicine Health Science and Technology Program (2022RC209) and Basic Public Welfare Research Project of Zhejiang Province (LQ24H060008 and LTGY23H060006).

Declaration of competing interest

The authors have no conflicts of interest relevant to this article.

Acknowledgements

We thank Scientific Research Center of Wenzhou Medical University for consultation and instrument availability that supported this work.

Abbreviations

Sip: sipeimine; **OA**: osteoarthritis; **ECM**: extracellular matrix; **LPS**: lipopolysaccharide; **MMP-13**: matrix metalloproteinase-13; **ADAMTS-5**: a disintegrin and metalloproteinase with thrombospondin motifs-5; **COX-2**: cyclooxygenase-2; **iNOS**: inducible nitric oxide synthase; **NLRP3**: nod-like receptor pyrin domain 3; **ASC**: apoptosis-associated speck-like protein; **NF-κB**: nuclear factor-κB; **GSDMD**: Gasdermin D; **DMM**: medial meniscus surgical destabilization; **PI3K**: phosphatidylinositol 3-kinase; **AKT**: protein kinase B; **LDH**: lactate dehydrogenase; **OARSI**: International Osteoarthritis Research Society.

References

[1] Wang BW, Jiang Y, Yao ZL, Chen PS, Yu B, Wang SN. Aucubin protects chondrocytes against IL-1beta-induced apoptosis in vitro and inhibits osteoarthritis in mice model. Drug Des Devel Ther 2019;13:3529–38. https://doi.org/10.2147/DDDT.S210220.

[2] Cui J, Shibata Y, Zhu T, Zhou J, Zhang J. Osteocytes in bone aging: advances, challenges, and future perspectives. Ageing Res Rev 2022;77:101608. https://doi.org/10.1016/j.arr.2022.101608.

[3] Rahmati M, Nalesso G, Mobasheri A, Mozafari M. Aging and osteoarthritis: central role of the extracellular matrix. Ageing Res Rev 2017;40:20–30. https://doi.org/10.1016/j.arr.2017.07.004.

[4] Rahmati M, Mobasheri A, Mozafari M. Inflammatory mediators in osteoarthritis: a critical review of the state-of-the-art, current prospects, and future challenges. Bone 2016;85:81–90. https://doi.org/10.1016/j.bone.2016.01.019.

[5] Kapoor M, Martel-Pelletier J, Lajeunesse D, Pelletier JP, Fahmi H. Role of proinflammatory cytokines in the pathophysiology of osteoarthritis. Nat Rev Rheumatol 2011;7(1):33–42. https://doi.org/10.1038/nrrheum.2010.196.
[6] Daheshia M, Yao JQ. The interleukin 1beta pathway in the pathogenesis of osteoarthritis. J Rheumatol 2008;35(12):2306–12. https://doi.org/10.3899/jrheum.080346.
[7] Jenei-Lanzl Z, Meurer A, Zaucke F. Interleukin-1beta signaling in osteoarthritis - chondrocytes in focus. Cell Signal 2019;53:212–23. https://doi.org/10.1016/j.cellsig.2018.10.005.
[8] de Lange-Brokaar BJ, Ioan-Facsinay A, van Osch GJ, Zuurmond AM, Schoones J, Toes RE, et al. Synovial inflammation, immune cells and their cytokines in osteoarthritis: a review. Osteoarthritis Cartilage 2012;20(12):1484–99. https://doi.org/10.1016/j.joca.2012.08.027.
[9] Miao EA, Rajan JV, Aderem A. Caspase-1-induced pyroptotic cell death. Immunol Rev 2011;243(1):206–14. https://doi.org/10.1111/j.1600-065X.2011.01044.x.
[10] Zhao LR, Xing RL, Wang PM, Zhang NS, Yin SJ, Li XC, et al. NLRP1 and NLRP3 inflammasomes mediate LPS/ATP-induced pyroptosis in knee osteoarthritis. Mol Med Rep 2018;17(4):5463–9. https://doi.org/10.3892/mmr.2018.8520.
[11] Zhou J, Zhao Y, Wu G, Lin B, Li Z, Liu X. Differential miRNAomics of the synovial membrane in knee osteoarthritis induced by bilateral anterior cruciate ligament transection in rats. Mol Med Rep 2018;18(4):4051–7. https://doi.org/10.3892/mmr.2018.9385.
[12] Chang SH, Mori D, Kobayashi H, Mori Y, Nakamoto H, Okada K, et al. Excessive mechanical loading promotes osteoarthritis through the gremlin-1-NF-kappaB pathway. Nat Commun 2019;10(1):1442. https://doi.org/10.1038/s41467-019-09491-5.
[13] Cao Y, Tang S, Nie X, Zhou Z, Ruan G, Han W, et al. Decreased miR-214-3p activates NF-kappaB pathway and aggravates osteoarthritis progression. EBioMedicine 2021;65:103283. https://doi.org/10.1016/j.ebiom.2021.103283.
[14] Wang Q, Ou Y, Hu G, Wen C, Yue S, Chen C, et al. Naringenin attenuates non-alcoholic fatty liver disease by down-regulating the NLRP3/NF-kappaB pathway in mice. Br J Pharmacol 2020;177(8):1806–21. https://doi.org/10.1111/bph.14938.
[15] McAllister MJ, Chemaly M, Eakin AJ, Gibson DS, McGilligan VE. NLRP3 as a potentially novel biomarker for the management of osteoarthritis. Osteoarthritis Cartilage 2018;26(5):612–9. https://doi.org/10.1016/j.joca.2018.02.901.
[16] Zhang C, Shao Z, Hu X, Chen Z, Li B, Jiang R, et al. Inhibition of PI3K/Akt/NF-kappaB signaling by Aloin for ameliorating the progression of osteoarthritis: in vitro and in vivo studies. Int Immunopharmacol 2020;89(Pt B):107079. https://doi.org/10.1016/j.intimp.2020.107079.
[17] Sun K, Luo J, Guo J, Yao X, Jing X, Guo F. The PI3K/AKT/mTOR signaling pathway in osteoarthritis: a narrative review. Osteoarthritis Cartilage 2020;28(4):400–9. https://doi.org/10.1016/j.joca.2020.02.027.
[18] Lin G, Li P, Li SL, Chan SW. Chromatographic analysis of Fritillaria isosteroidal alkaloids, the active ingredients of Beimu, the antitussive traditional Chinese medicinal herb. J Chromatogr A 2001;935(1–2):321–38. https://doi.org/10.1016/s0021-9673(01)01258-4.
[19] Wang D, Zhu J, Wang S, Wang X, Ou Y, Wei D, et al. Antitussive, expectorant and anti-inflammatory alkaloids from bulbus Fritillariae cirrhosae. Fitoterapia 2011;82(8):1290–4. https://doi.org/10.1016/j.fitote.2011.09.006.
[20] Lin Y, Yue H, Wang P, Zhang J, Jia Y, Chang S, et al. Advances in the study of anti-inflammatory effects of Fritillariae cirrhosae bulbus and its main components. Adv Clin Med 2023;13(6):10212–9. https://doi.org/10.12677/acm.2023.1361429.
[21] Kang DG, Sohn EJ, Lee YM, Lee AS, Han JH, Kim TY, et al. Effects of bulbus Fritillaria water extract on blood pressure and renal functions in the L-NAME-induced hypertensive rats. J Ethnopharmacol 2004;91(1):51–6. https://doi.org/10.1016/j.jep.2003.11.015.
[22] Wang DD, Feng Y, Li Z, Zhang L, Wang S, Zhang CY, et al. In vitro and in vivo antitumor activity of Bulbus Fritillariae Cirrhosae and preliminary investigation of its mechanism. Nutr Cancer 2014;66(3):441–52. https://doi.org/10.1080/01635581.2013.878737.
[23] Wang D, Du Q, Li H, Wang S. The isosteroid alkaloid imperialine from bulbs of Fritillaria cirrhosa mitigates pulmonary functional and structural impairment and suppresses inflammatory response in a COPD-like rat model. Mediat Inflamm 2016;2016:4192483. https://doi.org/10.1155/2016/4192483.
[24] Wu K, Mo C, Xiao H, Jiang Y, Ye B, Wang S. Imperialine and verticinone from bulbs of Fritillaria wabuensis inhibit pro-inflammatory mediators in LPS-stimulated RAW 264.7 macrophages. Planta Med 2015;81(10):821–9. https://doi.org/10.1055/s-0035-1546170.
[25] Huang D, Shen Z, Zhao S, Pei C, Jia N, Wang Y, et al. Sipeimine attenuates PM2.5-induced lung toxicity via suppression of NLRP3 inflammasome-mediated pyroptosis through activation of the PI3K/AKT pathway. Chem Biol Interact 2023;376:110448. https://doi.org/10.1016/j.cbi.2023.110448.
[26] Wang Y, Shen Z, Zhao S, Huang D, Wang X, Wu Y, et al. Sipeimine ameliorates PM2.5-induced lung injury by inhibiting ferroptosis via the PI3K/Akt/Nrf2 pathway: a network pharmacology approach. Ecotoxicol Environ Saf 2022;239:113615. https://doi.org/10.1016/j.ecoenv.2022.113615.
[27] Steibel JP, Poletto R, Coussens PM, Rosa GJ. A powerful and flexible linear mixed model framework for the analysis of relative quantification RT-PCR data. Genomics 2009;94(2):146–52. https://doi.org/10.1016/j.ygeno.2009.04.008.
[28] Lewis JS, Hembree WC, Furman BD, Tippets L, Cattel D, Huebner JL, et al. Acute joint pathology and synovial inflammation is associated with increased intra-articular fracture severity in the mouse knee. Osteoarthritis Cartilage 2011;19(7):864–73. https://doi.org/10.1016/j.joca.2011.04.011.
[29] Giorgino R, Albano D, Fusco S, Peretti GM, Mangiavini L, Messina C. Knee osteoarthritis: epidemiology, pathogenesis, and mesenchymal stem cells: what else is new? An update. Int J Mol Sci 2023;24(7). https://doi.org/10.3390/ijms24076405.
[30] Yao Q, Wu X, Tao C, Gong W, Chen M, Qu M, et al. Osteoarthritis: pathogenic signaling pathways and therapeutic targets. Signal Transduct Targeted Ther 2023;8(1):56. https://doi.org/10.1038/s41392-023-01330-w.
[31] Zeng C, Wei J, Persson MSM, Sarmanova A, Doherty M, Xie D, et al. Relative efficacy and safety of topical non-steroidal anti-inflammatory drugs for osteoarthritis: a systematic review and network meta-analysis of randomised controlled trials and observational studies. Br J Sports Med 2018;52(10):642–50. https://doi.org/10.1136/bjsports-2017-098043.
[32] Jiang RW, Ma SS, But PP, Dong H, Mak TC. Sipeimine, a steroidal alkaloid from Fritillaria roylei Hooker. Acta Crystallogr C 2001;57(Pt 2):170–1. https://doi.org/10.1107/s0108270100014499.
[33] Goldring MB, Otero M. Inflammation in osteoarthritis. Curr Opin Rheumatol 2011;23(5):471–8. https://doi.org/10.1097/BOR.0b013e328349c2b1.
[34] Wojdasiewicz P, Poniatowski LA, Szukiewicz D. The role of inflammatory and anti-inflammatory cytokines in the pathogenesis of osteoarthritis. Mediat Inflamm 2014;2014:561459. https://doi.org/10.1155/2014/561459.
[35] Kovacs B, Vajda E, Nagy EE. Regulatory effects and interactions of the wnt and OPG-RANKL-RANK signaling at the bone-cartilage interface in osteoarthritis. Int J Mol Sci 2019;20(18). https://doi.org/10.3390/ijms20184653.
[36] Rapp AE, Zaucke F. Cartilage extracellular matrix-derived matrikines in osteoarthritis. Am J Physiol Cell Physiol 2023;324(2):C377–94. https://doi.org/10.1152/ajpcell.00464.2022.
[37] Hao X, Zhao J, Jia L, He T, Wang H, Fan J, et al. XMU-MP-1 attenuates osteoarthritis via inhibiting cartilage degradation and chondrocyte apoptosis. Front Bioeng Biotechnol 2022;10:998077. https://doi.org/10.3389/fbioe.2022.998077.
[38] Long Y, Liu X, Tan XZ, Jiang CX, Chen SW, Liang GN, et al. ROS-induced NLRP3 inflammasome priming and activation mediate PCB 118- induced pyroptosis in endothelial cells. Ecotoxicol Environ Saf 2020;189:109937. https://doi.org/10.1016/j.ecoenv.2019.109937.
[39] Dong HC, Li PN, Chen CJ, Xu X, Zhang H, Liu G, et al. Sinomenine attenuates cartilage degeneration by regulating miR-223-3p/NLRP3 inflammasome signaling. Inflammation 2019;42(4):1265–75. https://doi.org/10.1007/s10753-019-00986-3.
[40] Joosten LA, Netea MG, Fantuzzi G, Koenders MI, Helsen MM, Sparrer H, et al. Inflammatory arthritis in caspase 1 gene-deficient mice: contribution of proteinase 3 to caspase 1-independent production of bioactive interleukin-1beta. Arthritis Rheum 2009;60(12):3651–62. https://doi.org/10.1002/art.25006.
[41] Clavijo-Cornejo D, Martinez-Flores K, Silva-Luna K, Martinez-Nava GA, Fernandez-Torres J, Zamudio-Cuevas Y, et al. The overexpression of NALP3 inflammasome in knee osteoarthritis is associated with synovial membrane prolidase and NADPH oxidase 2. Oxid Med Cell Longev 2016;2016:1472567. https://doi.org/10.1155/2016/1472567.
[42] Zheng X, Zhong T, Ma Y, Wan X, Qin A, Yao B, et al. Bnip3 mediates doxorubicin-induced cardiomyocyte pyroptosis via caspase-3/GSDME. Life Sci 2020;242:117186. https://doi.org/10.1016/j.lfs.2019.117186.
[43] Liu Z, Yao X, Jiang W, Li W, Zhu S, Liao C, et al. Advanced oxidation protein products induce microglia-mediated neuroinflammation via MAPKs-NF-kappaB signaling pathway and pyroptosis after secondary spinal cord injury. J Neuroinflammation 2020;17(1):90. https://doi.org/10.1186/s12974-020-01751-2.
[44] Hu J, Zhou J, Wu J, Chen Q, Du W, Fu F, et al. Loganin ameliorates cartilage degeneration and osteoarthritis development in an osteoarthritis mouse model through inhibition of NF-kappaB activity and pyroptosis in chondrocytes. J Ethnopharmacol 2020;247:112261. https://doi.org/10.1016/j.jep.2019.112261.
[45] Tian Y, Feng X, Zhou Z, Qin S, Chen S, Zhao J, et al. Ginsenoside compound K ameliorates osteoarthritis by inhibiting the chondrocyte endoplasmic reticulum stress-mediated IRE1alpha-TXNIP-NLRP3 Axis and pyroptosis. J Agric Food Chem 2023;71(3):1499–509. https://doi.org/10.1021/acs.jafc.2c06134.
[46] Yan Z, Qi W, Zhan J, Lin Z, Lin J, Xue X, et al. Activating Nrf2 signalling alleviates osteoarthritis development by inhibiting inflammasome activation. J Cell Mol Med 2020;24(22):13046–57. https://doi.org/10.1111/jcmm.15905.
[47] Li C, Wang X, Kuang M, Li L, Wang Y, Yang F, et al. UFL1 modulates NLRP3 inflammasome activation and protects against pyroptosis in LPS-stimulated bovine mammary epithelial cells. Mol Immunol 2019;112:1–9. https://doi.org/10.1016/j.molimm.2019.04.023.
[48] Liang Y, Chen S, Yang Y, Lan C, Zhang G, Ji Z, et al. Vasoactive intestinal peptide alleviates osteoarthritis effectively via inhibiting NF-kappaB signaling pathway. J Biomed Sci 2018;25(1):25. https://doi.org/10.1186/s12929-018-0410-z.
[49] Zhang D, Cao X, Li J, Zhao G. MiR-210 inhibits NF-kappaB signaling pathway by targeting DR6 in osteoarthritis. Sci Rep 2015;5:12775. https://doi.org/10.1038/srep12775.
[50] Yang G, Wang Y, Chen Y, Huang R. UFL1 attenuates IL-1beta-induced inflammatory response in human osteoarthritis chondrocytes. Int Immunopharmacol 2020;81:106278. https://doi.org/10.1016/j.intimp.2020.106278.
[51] Choi MC, Jo J, Park J, Kang HK, Park Y. NF-kappaB signaling pathways in osteoarthritic cartilage destruction. Cells 2019;8(7). https://doi.org/10.3390/cells8070734.
[52] Wang C, Zeng L, Zhang T, Liu J, Wang W. Tenuigenin prevents IL-1beta-induced inflammation in human osteoarthritis chondrocytes by suppressing PI3K/AKT/NF-kappaB signaling pathway. Inflammation 2016;39(2):807–12. https://doi.org/10.1007/s10753-016-0309-3.

[53] Jiang RH, Xu JJ, Zhu DC, Li JF, Zhang CX, Lin N, et al. Glycyrrhizin inhibits osteoarthritis development through suppressing the PI3K/AKT/NF-kappaB signaling pathway in vivo and in vitro. Food Funct 2020;11(3):2126–36. https://doi.org/10.1039/c9fo02241d.

[54] Ji B, Zhang Z, Guo W, Ma H, Xu B, Mu W, et al. Isoliquiritigenin blunts osteoarthritis by inhibition of bone resorption and angiogenesis in subchondral bone. Sci Rep 2018;8(1):1721. https://doi.org/10.1038/s41598-018-19162-y.

[55] Lin C, Liu L, Zeng C, Cui ZK, Chen Y, Lai P, et al. Activation of mTORC1 in subchondral bone preosteoblasts promotes osteoarthritis by stimulating bone sclerosis and secretion of CXCL12. Bone Res 2019;7(5). https://doi.org/10.1038/s41413-018-0041-8.

[56] Hu X, Ji X, Yang M, Fan S, Wang J, Lu M, et al. Cdc42 is essential for both articular cartilage degeneration and subchondral bone deterioration in experimental osteoarthritis. J Bone Miner Res 2018;33(5):945–58. https://doi.org/10.1002/jbmr.3380.